TECTONIC IMPLICATIONS OF PALEOPROTEROZOIC STRUCTURE AND METAMORPHISM IN THE NORTHERN HUALAPAI MOUNTAINS, MOHAVE COUNTY, ARIZONA

By Benjamin R. Siwiec

A Thesis

Submitted in Partial Fulfillment

of the Requirements for the Degree of

Master of Science

in Geology

Northern Arizona University

December 2003

Approved:

_____

Ernest M. Duebendorfer, Ph.D., Chair

_____

Thomas D. Hoisch, Ph.D.

_____

Paul J. Umhoefer, Ph.D.

ABSTRACT

Tectonic implications of Paleoproterozoic structure and metamorphism in the northern Hualapai Mountains, Mohave County, Arizona

Benjamin R. Siwiec

The Hualapai Mountains have previously been considered to be part of the isotopically mixed boundary zone between the Mojave and Yavapai Proterozoic crustal provinces in Arizona. The western margin of this boundary zone has been proposed to trend southwest from the Gneiss Canyon shear zone in the Lower Granite Gorge of the Grand Canyon through the northern Hualapai Mountains. Mapping, structural analysis, and metamorphic studies in the northern Hualapai Mountains indicate that this may not be the case. This study also documents a previously unrecognized deformational fabric temporally intermediate between the two Paleoproterozoic deformational events recorded in Arizona. The regional D_1, represented by a northwest-striking foliation and dated elsewhere in Arizona at 1740-1720 Ma, remains unchanged. The regional deformation previously referred to as D_2 (1700-1690 Ma), represented by a steeply dipping northeast-striking foliation, is renamed D_3. The temporally intermediate fabric, referred to as S_2, consists of a post-1717 Ma north- to northwest-striking foliation and fold axes that overprint the S_1 fabric, but are reoriented by S_3. The two previously recognized fabrics are identical to those preserved in the Cerbat Mountains, across the proposed southwest projection of the Gneiss Canyon shear zone. The Gneiss Canyon shear zone has been described as an 11-km wide, highly migmatitic, D_2 shear zone characterized by LS fabrics with strong northwest-side-up kinematic indicators. In contrast, in the northern

Hualapai Mountains, domains of D_3 deformation are narrower, significant areas of D_1 fabric are preserved, very few rocks are migmatitic, S tectonite fabrics are dominant (suggesting flattening strains), and very few kinematic indicators are present. In the Lower Granite Gorge, the Gneiss Canyon shear zone separates granulite facies rocks (650-700^{o}C and 3.5-4.5 kb) to the northwest from amphibolite facies rocks (550-600^{o}C and 2.3-3.5 kb) to the southeast, whereas rocks within and to the south of the present study area are granulite facies (650-720^{o} C and 5.1-6.2 kb) and only slightly lower grade than the Cerbat Mountains. This observation is compatible with recent metamorphic work in the Peacock Mountains and Pb isotopic studies that place the western margin of the boundary zone significantly east of the Hualapai Mountains.

ACKNOWLEDGMENTS

First and foremost, I need to thank my advisor, Ernie Duebendorfer, for all the time and effort (and funding) he has invested in me and my project. Without Ernie's trips to help me in the field and his numerous revisions of my thesis chapters, this project almost certainly would not have worked out. Paul Umhoefer deserves thanks for his insightful discussions of tectonics and his unfaltering drive to compare Paleoproterozoic events with modern-day tectonics and basins. I'd like to thank Tom Hoisch for his help with all the metamorphic aspects of my thesis and especially for his help with the GASP and garnet-biotite analysis software. Thank you, Jim Wittke for your help with the electron microprobe and the discussions that took place while the probe was running.

I need to thank Gwyn Rhys-Evans, who was writing a senior thesis on rocks adjacent to mine, for the useful information I learned from his work and for having someone to hang out with in the desert. Thanks also to my field assistants, Rusty Rigg, Janelle Sikorski, and Travis Loseke, some of whom may have redefined suffering while in my field area. Karl Karlstrom deserves special thanks for his discussions about Paleoproterozoic geology and for taking me on a research trip on the Colorado, a priceless experience. Kevin Chamberlain also deserves thanks for "rushing" me a zircon date. Lastly, I need to thank my brother Tim for sneaking into the GSA meeting in Seattle to see my talk, even though without a geology background it couldn't have made much sense to him.

Thank you to the groups that provided funding for this project: National Science Foundation grant #EAR-0001241, Geological Society of America research grant, Arizona Geological Society Courtright scholarship, and the Friday Lunch Clubbe.

TABLE OF CONTENTS

LIST OF TABLES

LIST OF FIGURES

LIST OF PLATES

CHAPTER 1: INTRODUCTION

Background

During the past 20 years, increasing attention has focused on Proterozoic crustal growth in the southwestern United States. The assembly of the Archean Wyoming province was complete by the early Paleoproterozoic and a passive margin existed along its southern margin by about 2.0 Ga (Karlstrom and Houston, 1984). The basement rocks of the southwest were accreted to the Wyoming province between 1.8 and 1.6 Ga and a series of accretionary events added 1200 km of crust to the expanding craton (Karlstrom and Houston, 1984; Duebendorfer and Houston, 1987). Island arc terranes were first sutured to the southern margin of the Wyoming province during the Medicine Bow orogeny (1780-1760 Ma) along the Cheyenne Belt in southern Wyoming and northern Colorado (Karlstrom and Houston, 1984; Duebendorfer and Houston, 1987; Chamberlain, 1998). The Paleoproterozoic rocks of Arizona were subsequently accreted to the southern margin of the older Paleoproterozoic rocks of Colorado and Utah between 1710 and 1680 Ma (Duebendorfer et al., 2001a; Figure 1).

The events outlined above are analogous to a more recent and better understood tectonic setting. They are directly analogous to the accretionary events that built up the western margin of the North American continent largely during the Mesozoic. During that time, most of the material that now makes up the states of Washington, Oregon, California, and Alaska, along with much of British Columbia and Yukon was accreted in several distinct orogenic pulses.

Northwestern Arizona experienced very little deformation during the nearly 1.6 billion years following the accretion of Paleoproterozoic rocks. During the

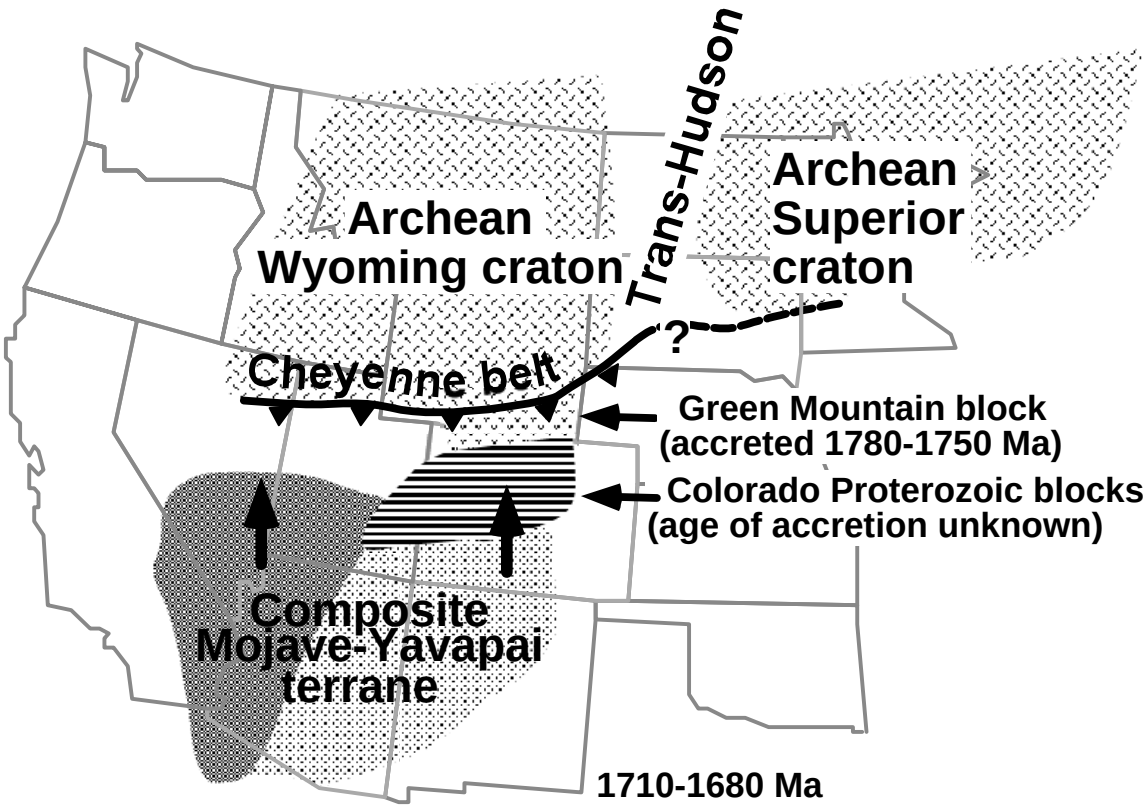

Figure 1. Overview map showing Paleoproterozoic and older rocks of the western United States. Shapes of tectonic blocks and arrows showing accretion direction are schematic. The study area was accreted to the craton between 1710 and 1680 Ma as part of the composite Mojave-Yavapai terrane.

Mesoproterozoic, the area was intruded by the continent-wide belt of A-type granitoid plutons (Emslie, 1978; Anderson and Bender, 1989; Windley, 1993), but deformation was largely localized and in many cases the granites intruded along pre-existing Paleoproterozoic trends (Ferguson, 2002). The rocks of western Arizona were not deformed by the Mesoproterozoic Grenville orogeny, or any of the Paleozoic orogenies (Antler, Sonoma, and Ancestral Rockies) and were apparently not deformed until the Laramide orogeny, when plutons (65-72 Ma) intruded north and east of the Cerbat Mountains (Young, 1979).

Proterozoic rocks in northwestern Arizona were exposed at the surface by the Cambrian when the Tapeats Sandstone was deposited on them. These rocks may have also been exposed prior to that, when the rocks of the Grand Canyon Supergroup were deposited on the Paleoproterozoic rocks of the eastern Grand Canyon, however, no evidence of such a depositional episode exists in northwestern Arizona. The Paleozoic and Mesozoic rocks that were deposited unconformably on the Proterozoic rocks were stripped off during Laramide time and the Proterozoic rocks were exposed again at the surface in the Paleocene as a result of broad Laramide uplifts at the incipient Colorado Plateau margin (Young, 1979). A long period of erosion must have followed, after which little topography remained because the 18.5 Ma Peach Springs tuff was deposited on a gently sloping surface with little relief between Kingman and the Colorado Plateau (Young and Brennan, 1974; Nielson et al., 1990). Tertiary sedimentary rocks north and east of Lake Mead were deposited on flat terrain and are no older than about 26 Ma (Bohannon, 1984; Beard, 1996). In the study area, the Peach Springs tuff and associated volcanic flows are nearly horizontal, indicating that, although areas to the west were

faulted and tilted by Basin and Range extension, the study area was largely spared from this deformation. Therefore, pre-Tertiary rocks in the study area have been little affected by Tertiary events. The consistency in orientations of fabrics in the study area with those found on the undeformed Colorado Plateau suggests that Paleoproterozoic orientations have been preserved regionally.

Three isotopically distinct provinces, the Mojave, Yavapai, and Mazatzal (from west to east), have been defined in Arizona (Figure 2). The Mojave province is the oldest and contains plutonic rocks with maximum crystallization ages of 1783±12 Ma (Baldwin Lake gneiss, Barth et al., 2000). The Elves Chasm pluton in the Upper Granite Gorge of the Grand Canyon has a crystallization age of 1840±1 Ma and is the oldest rock with a Mojave province Pb isotopic signature (Hawkins et al, 1996), but it lies within the Mojave-Yavapai boundary zone (discussed below). Detrital zircons from metasedimentary rocks in the Mojave province have yielded late Archean ages (as old as 2600 Ma, Wooden et al., 1994), indicating that there may have been an Archean component in the original sediments of the Mojave province, although no rocks with Archean crystallization ages have been found. Regardless of the presence of Archean rocks within the Mojave province, the zircon ages indicate that the Mojave province had an older provenance to supply the older zircons. This would likely have been an Archean continental source.

The Yavapai province in Arizona consists of juvenile volcanic arc rocks and tectonically related granitoids that do not contain the older crustal component found in the Mojave province. Yavapai province rocks are ca. 1.76 to 1.70 Ga and were accreted to the growing North American craton between 1.71 and 1.68 Ga (Karlstrom and

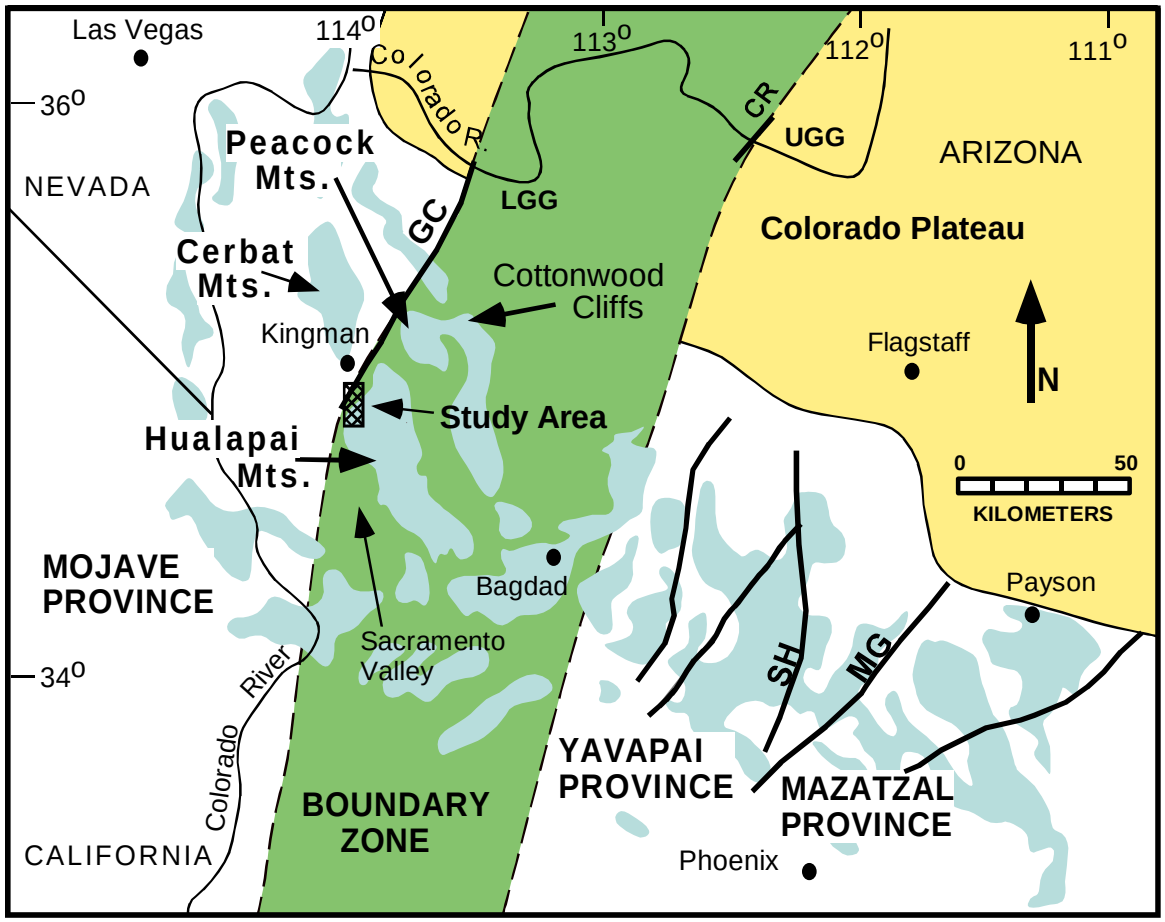

Figure 2. Generalized map showing the Mojave, Yavapai, and Mazatzal Proterozoic provinces in Arizona. The map also shows the previously proposed boundary zone between the Mojave and Yavapai provinces. Abbreviations: CR: Crystal shear zone; GC: previously proposed trace of the Gneiss Canyon shear zone; LGG: Lower Granite Gorge of the Grand Canyon; MG: Moore Gulch shear zone; SH: Shylock shear zone; UGG: Upper Granite Gorge of the Grand Canyon.

Bowring, 1988). The Mazatzal province is exposed in central and eastern Arizona and also consists of juvenile volcanic arc rocks and associated granitoids as old as 1.75 to 1.76 Ga (Karlstrom and Bowring, 1993) and younger sedimentary sequences. It contains a 1.73 Ga ophiolite (Payson ophiolite) with an isotopic signature indicating an older crustal component is present. It was upon this ophiolite that the sedimentary rocks of the Mazatzal province were deposited (Dann, 1997).

The boundary between the Yavapai and Mazatzal provinces is considered to be the Moore Gulch shear zone in central Arizona (Figure 2), which is buried beneath the Phanerozoic rocks of the Colorado Plateau to the northeast. This boundary has been traced across the Colorado Plateau and into New Mexico as the Jemez lineament (Karlstrom and the CD-ROM Working Group, 2002). The boundary between the Mojave and Yavapai province was once proposed to be represented by the northeast-striking Gneiss Canyon shear zone in the Lower Granite Gorge of the Grand Canyon, but isotopic studies have since shown that the boundary may not be fully represented by a single, narrow feature (Wooden and DeWitt, 1991).

A poorly understood area of mixed isotopic (Pb) character approximately 75 km wide (Figure 3) has been discovered between crust that has definitively Mojave or Yavapai Pb isotope values (Wooden and DeWitt, 1991). This area has been proposed to represent a crustal boundary zone between the Mojave and Yavapai provinces in northwestern Arizona. The eastern margin of this zone is defined by a steep gradient in Pb isotope values near Bagdad, Arizona (Wooden and DeWitt, 1991), and appears to coincide with the Crystal shear zone in the Upper Granite Gorge of the Grand Canyon (Hawkins et al., 1996). The western margin has been proposed to be the Gneiss Canyon

shear zone in the Lower Granite Gorge of the Grand Canyon based largely on perceived differences in metamorphism and fabrics across the area in the Lower Granite Gorge (Albin and Karlstrom, 1991). The Gneiss Canyon shear zone is an 11 km-wide northeast-striking structure containing strong northwest-side-up kinematic indicators (Karlstrom and Morgan, 1988).

The Gneiss Canyon shear zone (and the western margin of the boundary zone) has been projected southwest from the Lower Granite Gorge for at least 60 km because strong northeast-striking foliations present in the southern Grand Wash Cliffs and Peacock Mountains are parallel to and lie along strike with shear zone foliations in the Lower Granite Gorge (Albin, 1991). The Gneiss Canyon shear zone has been further proposed to continue through the northern Hualapai Mountains near Kingman, Arizona (Albin and Karlstrom, 1991). However, Pb isotopic data suggest that both the northern Hualapai Mountains and Cerbat Mountains (to the north) are wholly Mojave in isotopic character (Figure 3; Wooden and DeWitt, 1991; K. Chamberlain, personal communication to E. Duebendorfer, 1999-2001), eliminating the need for an isotopic boundary between them. This study evaluates the possibility that the Gneiss Canyon shear zone is present in the northern Hualapai Mountains.

The Gneiss Canyon shear zone has also been proposed as the boundary between granulite facies (to the northwest) and amphibolite facies rocks (to the southeast) in northwestern Arizona (Albin and Karlstrom, 1991; Robinson, 1994). Reconnaissance work conducted prior to this thesis indicated that at least some pelitic rocks in the northern Hualapai Mountains contain granulite facies assemblages and preliminary thermobarometry on one sample from the northern Hualapai Mountains suggests

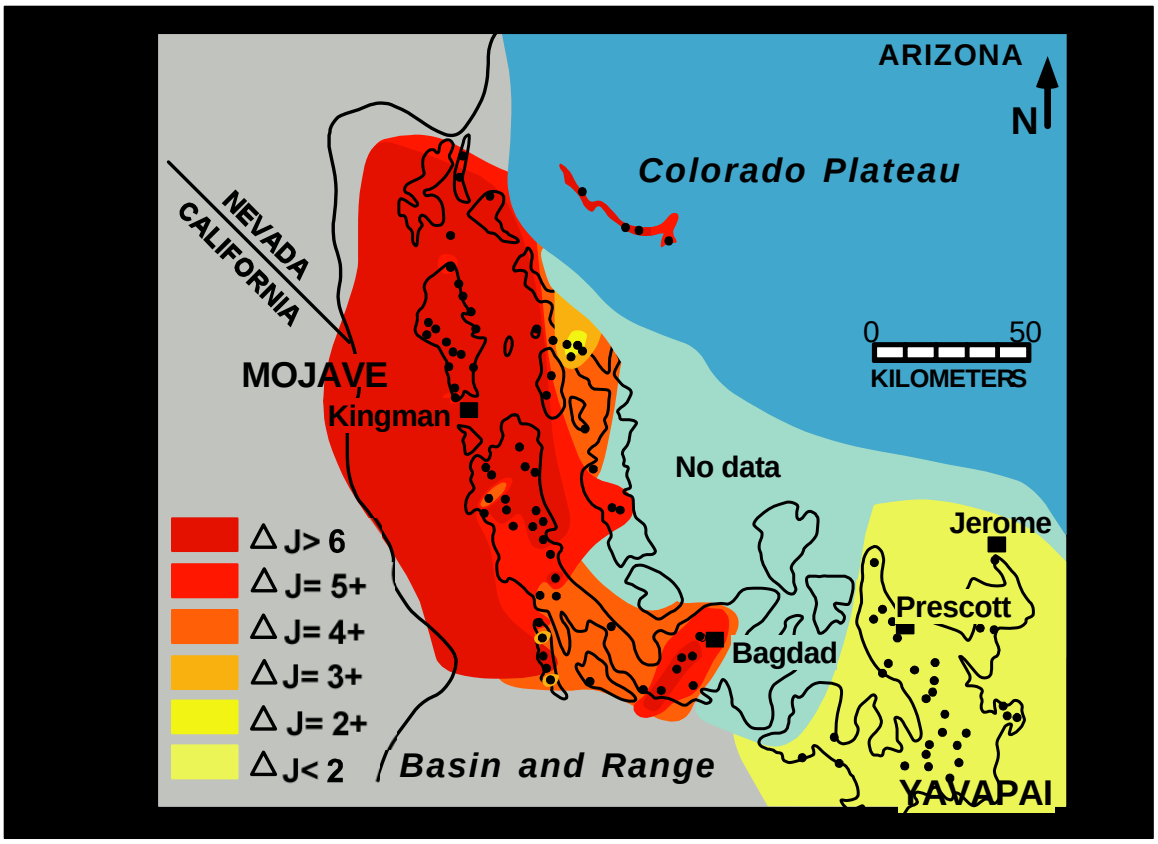

Figure 3. Map showing Pb isotope values after Wooden and DeWitt (1991) and modified with data from K. Chamberlain (personal communication to E. Duebendorfer, 1999-2001). Delta Jerome (Δ J) values indicate the variance in $^{207}Pb/^{204}Pb$ isotopic signature compared with data from Jerome, Arizona, which is considered to be in the Yavapai province. Rocks of the Mojave province yield higher values than those from the Yavapai province. Note that data collected near the study area, immediately south of Kingman, has yielded delta Jerome values that are wholly Mojave-like in character. Also note the prominent isotopic gradient to the east of Kingman.

metamorphism at 630^{o} C and 5.6 kb (Duebendorfer et al., 2001b). Because these pressures are similar to those obtained from the Cerbat Mountains (although the temperatures are slightly lower, Jones, 1998) there is some question whether or not there is a sharp metamorphic boundary between the Hualapai and Cerbat ranges. The metamorphic component of this study was designed to test the hypothesis that a metamorphic boundary lies between the two ranges by comparing metamorphism in the northern Hualapai Mountains with that reported from the Cerbat Mountains (Jones, 1998; Duebendorfer et al., 2001a).

Two penetrative Proterozoic fabrics have been recognized in Arizona (e.g., Karlstrom and Bowring, 1988; Duebendorfer et al., 2001a), both of which are present in the study area. The younger is a northeast-striking, subvertical foliation associated with the regional "D_2 event" at 1700-1690 Ma and is considered by most workers to have formed as a result of the accretion of the Arizona Proterozoic terranes to the growing Proterozoic craton in western North America. This event is referred to as the Yavapai orogeny in Arizona and the Ivanpah orogeny in California (Karlstrom and Bowring, 1988). An older fabric, related to D_1, is bracketed between 1740-1720 Ma and is not as well understood because few places in northwestern Arizona preserve the D_1 fabric. A component of this study was to identify and characterize areas of northwest-striking D_1 fabric and study its relationship to the northeast-striking D_2 fabric, as well as identify any other fabrics encountered.

Methods

A north-south transect that extends south of Kingman to the Walnut Creek area was selected for study because field reconnaissance indicated the presence of both D_1 and D_2 fabrics, as well as pelitic rocks that could constrain the pressure and temperature of metamorphism. I mapped a 14 x 6 km transect at 1:12,000 scale and conducted structural analysis at the macroscopic and mesoscopic scales. In the laboratory, I analyzed aerial photographs to define large-scale structures and used the petrographic microscope to: (1) determine stable mineral assemblages for each deformational event, (2) study porphyroblast-matrix relationships to establish the relation and timing between metamorphism and deformation, and (3) establish kinematics of any shear zones encountered using the techniques summarized by Passchier and Trouw (1996).

My preliminary reconnaissance indicated that thermobarometry would be possible on pelitic assemblages (sillimanite – potassium feldspar – garnet – biotite – plagioclase) using GASP geobarometry (Holdaway, 2001), and the garnet-biotite geothermometer of Holdaway (2000). Some pelitic assemblages found within the study area proved to be unsuitable for the GASP method, but one outcrop produced suitable mineralogy for geobarometry. The Cameca MBX microprobe at Northern Arizona University was used to analyze mineral compositions. I collected 50 samples for petrographic and microstructural analysis and 5 samples for thermobarometry.

The products of this research are: (1) a 1:12,000-scale geologic map (Plate 1), (2) a structural form surface map (Plate 2), (3) a summary of kinematics of shear zones, (4) a quantitative pressure-temperature estimate of metamorphism using petrogenetic grids and thermobarometry, (5) a characterization of the geometry and kinematics of D_1 structures,

and (6) an evaluation of the presence of the western margin of Mojave-Yavapai boundary zone in the northern Hualapai Mountains.

CHAPTER 2: DESCRIPTION OF ROCK UNITS

Introduction

The study area is dominated by Quaternary valley fill, Tertiary volcanic rocks, and Proterozoic metamorphic and plutonic rocks. In most areas, the Proterozoic rocks occupy a space between the Quaternary sediments of the Sacramento Valley (Figure 2) on the west and the Tertiary volcanic rocks of the lower Hualapai Mountains on the east. Ten units have been identified for mapping purposes.

The geographical layout of the study area allows a natural division between a northern and a southern half. The northern half is dominated by two Paleoproterozoic units, granite (Xgr), and migmatitic gneiss (Xmg), and a Mesoproterozoic megacrystic granite (Ygr). South of the large dividing ridge of Tertiary volcanic rocks are the Paleoproterozoic units metasedimentary schist (Xms), orthogneiss (Xog), and amphibolite (Xam). The southern boundary of the study area is north of Walnut Creek. The other major geographic feature in the southern part of the study area is a large wash slightly south of the large dividing ridge called Shingle Canyon.

Units will be discussed from oldest to youngest, then from north to south where ages are similar or relative ages are unknown. The first group to be discussed will be metamorphic rocks, followed by metamorphosed plutonic rocks, and finally unmetamorphosed units.

Metamorphic Rocks

Paleoproterozoic Migmatitic Gneiss (Xmg)

Macroscopic Description and Field Relations

Paleoproterozoic migmatitic gneiss is exposed in the northern part of the study area, south of the Holy Moses mine. It is generally a strongly foliated, fine- to medium-grained gneiss consisting of quartz, K-feldspar, plagioclase, and biotite. It is exposed on steep slopes and in valleys between the Quaternary sediments on the west and the Tertiary volcanic rocks on the east. This unit is locally migmatitic, although it has not been possible to evaluate whether the migmatites are injection-related or anatectic. The migmatites contain some features suggestive partial melting such as elongate bodies and veins suggestive of leucosome and melanosome pairs (Figure 4), however, since the presence of melt-related structures cannot be confirmed, I infer that the temperature conditions of the migmatitic gneiss unit have not exceeded the melt threshold.

The migmatitic gneiss contains a strong northeast-striking and steeply-dipping foliation, but generally lacks a lineation. Mylonitic zones are also present, although many contain no lineation, making determination of sense of shear impossible. In areas of lower strain, this unit appears similar to the metasedimentary schist unit (Xms, described below) and in a few areas, the amphibolite unit (both of which are common in the southern part of the study area). Pegmatite dikes and veins are locally pervasive and this unit is also intruded in some areas by the Mesoproterozoic granite unit. The type of contact between the migmatitic gneiss and the granite (Xgr) to the north is difficult to locate precisely, because the two units interfinger and the granite unit contains large

Figure 4. Field photograph showing migmatitic texture in migmatitic gneiss. Note the separation of leucosome and melanosome pairs throughout the outcrop. View is obliquely downward and pencil for scale is 15 cm long.

xenoliths of the migmatitic gneiss. Their contact on the map is based on the relative abundance of the two units.

Microscopic Descriptions

The mineralogy of the migmatitic gneiss consists of, in decreasing abundance, quartz, K-feldspar, then lesser amounts of plagioclase, biotite, and hornblende (Figure 5). Tourmaline and sphene are also found in small amounts. Texture is fine to medium grained and schistose, except in migmatitic or mylonitic areas. Foliation is generally defined by preferred orientation of biotite grains, but also by compositional banding and a grain-shape fabric in some migmatitic or highly strained rocks. As with the mesoscopic scale, shear sense is not clearly discernible at the microscopic scale. Some mylonitic samples show asymmetric porphyroblasts, but with no reliable lineation, kinematics cannot be determined.

Interpretation

The mineralogic similarities to rocks found farther south (discussed below) indicates that this unit may be a northern extension of the metasedimentary schist unit (Xms), but more highly strained. Tertiary volcanic rocks comprise a large ridge that separates the migmatitic gneiss and metasedimentary schist and covers the contact between these units. Xenoliths of migmatitic gneiss within the granite (Xgr) to the north indicate that the unit is older than the granite. The majority of the migmatitic gneiss is

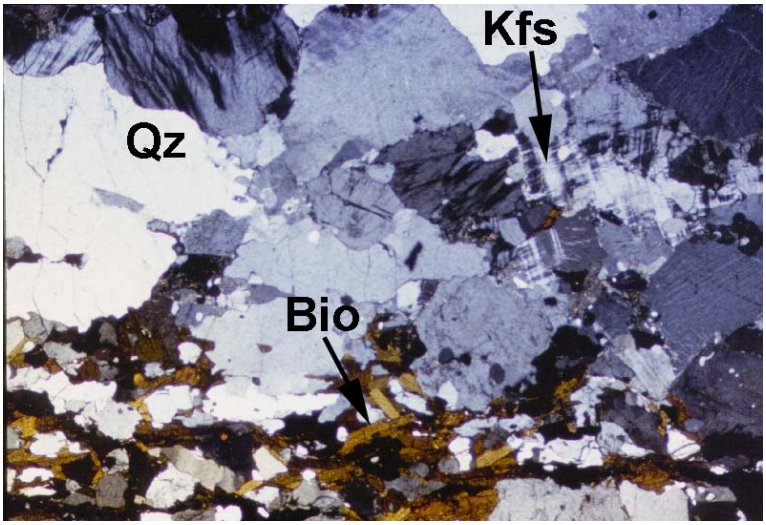

Figure 5. Photomicrograph of migmatitic gneiss in cross-polarized light containing quartz (Qz), K-feldspar (Kfs), and biotite (Bio). This sample contains a high temperature mylonitic fabric with dynamically recrystallized K-feldspar and quartz. View is 7 mm across the long dimension of the slide.

very rich in quartz and has a recrystallized texture bearing little resemblance to granitic rocks in the area. This unit is interpreted to consist of highly strained metasedimentary and metavolcanic rocks that have either been partially melted, intruded by dikes and veins, or both.

Paleoproterozoic Metasedimentary Schist (Xms)

Macroscopic Description and Field Relations

The metasedimentary schist unit is the dominant Proterozoic rock in the southern part of the study area. Most of its exposures are north of Walnut Creek and south of Shingle Canyon. The metasedimentary schist unit is a heterogeneous suite of rocks including psammitic and pelitic schists, amphibolite, and metamorphosed plutonic rocks. Due to the gradational nature of lithologic changes or extreme mixing (due to intrusion or intense transposition) of units at a scale too small to map, the above lithologies were combined into a single map unit. The primary rock type is schist consisting of quartz, K-feldspar, plagioclase, biotite, and in some areas, hornblende (Figure 6). It forms steep slopes and sharp ridges as well as large inselbergs (30-150 m high) within Quaternary deposits. This unit is capped in many areas by Tertiary volcanic rocks (Tv).

The most abundant mineral in the schist is quartz, but it also contains a large percentage of K-feldspar and lesser amounts of plagioclase and biotite. In some areas it contains garnet and/or hornblende. The schist generally has a strong foliation of variable strike defined by alignment of biotite grains in hand sample. The foliation dips steeply

Figure 6. Field photograph showing metasedimentary schist viewed parallel to northeast-striking steeply dipping foliation. View is straight down at horizontal outcrop with pencil (15 cm) for scale.

and locally contains a lineation. Shear sense indicators are limited, but present in some mylonite zones.

Two localities in the study area contain pelitic schist. In the southernmost part of the study area, at station 47 (Plate 3), there is one small area of pelitic schist. The rock has the typical metasedimentary schist mineralogy described above, but contains sillimanite that forms white bladed masses, garnet porphyroblasts that are 1-2 cm in diameter, and lacks hornblende (Figure 7). At station 59 (Plate 3), northwest of the first pelitic schist location, another outcrop contains pelitic schist composed of K feldspar, quartz, plagioclase, biotite, sillimanite, and garnet.

Lenses and larger elongate bodies of amphibolite too small to show on the map are common within the metasedimentary schist unit. For a description of amphibolite, please see the amphibolite (Xam) rock description.

Veins and elongate bodies of plutonic rocks up to 100 m wide are present within the metasedimentary schist unit. These are granitic and vary from fine grained to pegmatitic. They are foliated with strike of foliation parallel to that in the adjacent metasedimentary schist unit. Granitic rocks within the metasedimentary schist appear to be equivalent to the granitic rocks of the orthogneiss unit (Xog, described below). All rock types within the metasedimentary schist unit are intruded by pegmatitic veins that exhibit variable strikes.

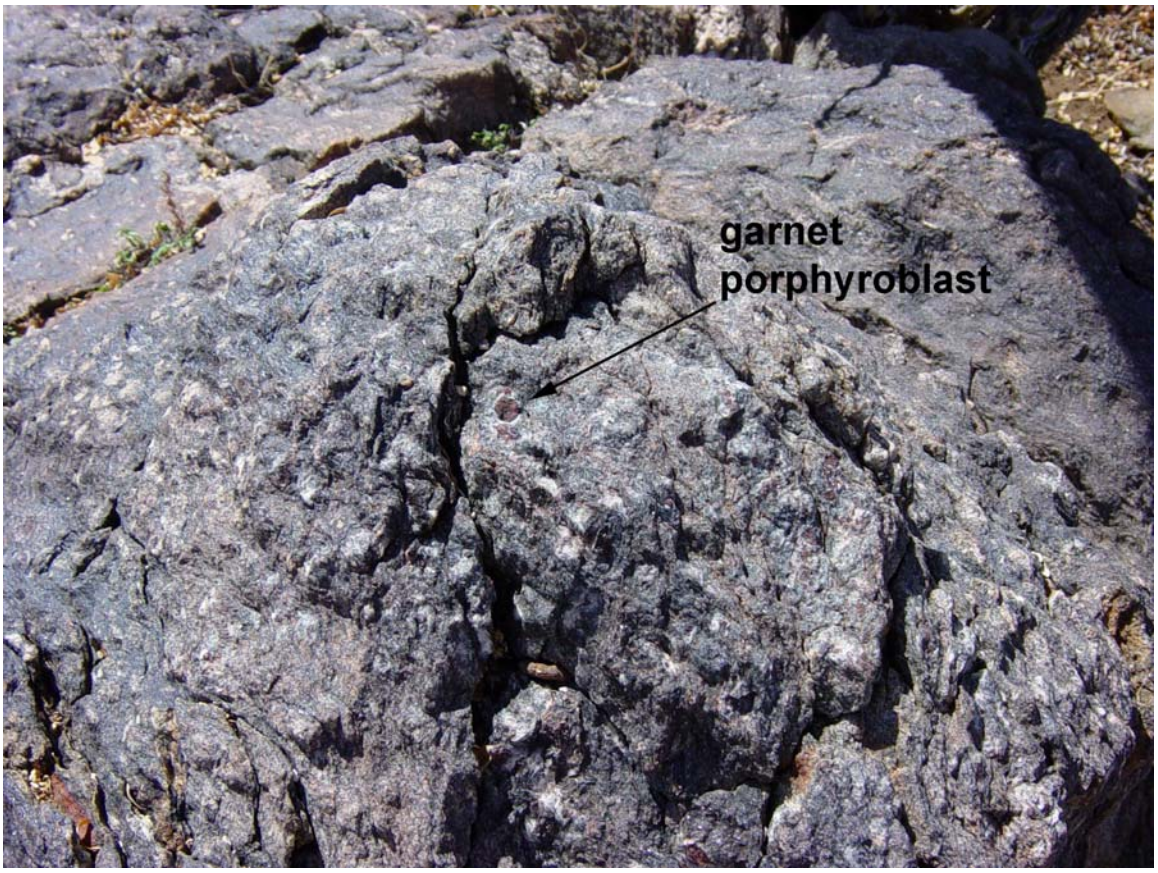

Figure 7. Field photograph showing pelitic schist within metasedimentary schist unit. This outcrop contains white sillimanite pods and large garnet porphyroblasts. The prominent garnet porphyroblast in the center of the photo is approximately 2 cm in diameter. View is oblique at uneven surface.

Microscopic Descriptions

The schist of the metasedimentary schist unit is dominated by recrystallized quartz, commonly K-feldspar associated with sericite, and lesser biotite that defines the foliation. Most samples contain minor plagioclase and small amounts of hornblende. Garnet is present in a few areas, but is locally highly retrograded to minerals such as biotite and sericite. Other minerals include tourmaline, sphene and opaque minerals such as ilmenite and magnetite (Figure 8). None of the pelitic schist samples studied contain prograde muscovite.

The pelitic schist contains a texture similar to much of the schist, but hornblende is absent, sillimanite is present, and biotite is more abundant. Sillimanite appears as masses of long narrow needles oriented parallel to foliation and wrapped around garnets. This rock is rich in quartz and K-feldspar, but has little plagioclase. Plagioclase in the pelitic schist near station 47 was analyzed with the electron microprobe and is nearly end-member albite.

Interpretation

The abundance of quartz in the schist suggests that this rock was not plutonic, but sedimentary in origin. It was probably a compositionally immature sandstone, perhaps a feldspathic sandstone. The presence of amphibolite lenses and granitic rocks suggests that this unit may have been originally interbedded with volcanic rocks and later intruded by felsic plutonic rocks. The pelitic schist indicates that there were aluminous mud rocks

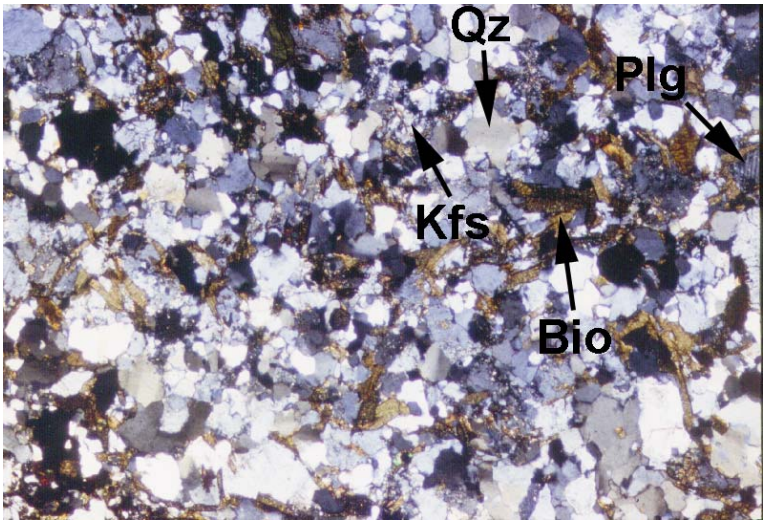

Figure 8. Photomicrograph showing typical mineralogy and texture of metasedimentary schist in cross-polarized light. Minerals include K feldspar (Kfs), plagioclase (Plg), biotite (Bio), and quartz (Qz). Note that foliation is difficult to discern in thin section. View is 3.5 mm across the long dimension of the slide.

in the depositional environment as well. These interpretations and the fact that the schist of this unit is quartz-rich suggest that these rocks were originally formed in a marine setting near a continental source. The lack of consistent strike of foliation and presence of fewer high-strain rocks such as mylonites suggest that this unit has undergone less strain than the migmatitic gneiss to the north.

Paleoproterozoic Amphibolite (Xam)

Macroscopic Description and Field Relations

The amphibolite is exposed as a narrow, elongate body adjacent to the metasedimentary schist unit and the orthogneiss unit (Xog). In some areas, the amphibolite lies between those units. It is generally 100 m wide or less, but traceable along strike for a distance of three or more kilometers. This unit is generally foliated, although the foliation is not as strong as in the adjacent rock. Lineations were not observed in the amphibolite. Foliation is mostly subparallel to adjacent to units and contacts, but in some areas foliation in the amphibolite strikes 90^{o} to foliation in adjacent units. The amphibolite unit forms slopes and is commonly traceable as a dark area between more resistant units.

The amphibolite has a simple mineralogy in most areas. It is primarily fine-grained hornblende and plagioclase that results in a salt-and-pepper texture. In one outcrop, garnet amphibolite was found.

Microscopic Descriptions

The garnet amphibolite consists primarily of cummingtonite, garnet, K-feldspar, plagioclase, and quartz, in decreasing order of abundance. The cummingtonite has a needle-like morphology. Foliation is not discernible in thin section (Figure 9). No thin sections of the amphibolite containing only amphibole and plagioclase were made.

Interpretation

The presence of amphibolite consisting of amphibole and plagioclase indicates that this unit is a metamorphosed mafic igneous rock, although it is not possible to discern whether the protolith was intrusive or extrusive. The presence of amphibolite lenses in the metasedimentary schist suggests that either the unit was deposited as basaltic flows interbedded with metasedimentary rocks or that it was injected as sills and/or dikes into the metasedimentary sequence. Therefore, the amphibolite is either coeval with or younger than the metasedimentary schist.

Metamorphosed Plutonic Rocks

Paleoproterozoic Granite (Xgr)

Macroscopic Description and Field Relations

The Paleoproterozoic granite is exposed in the northernmost part of the study area. It is a medium-grained quartzofeldspathic gneiss with a strong metamorphic

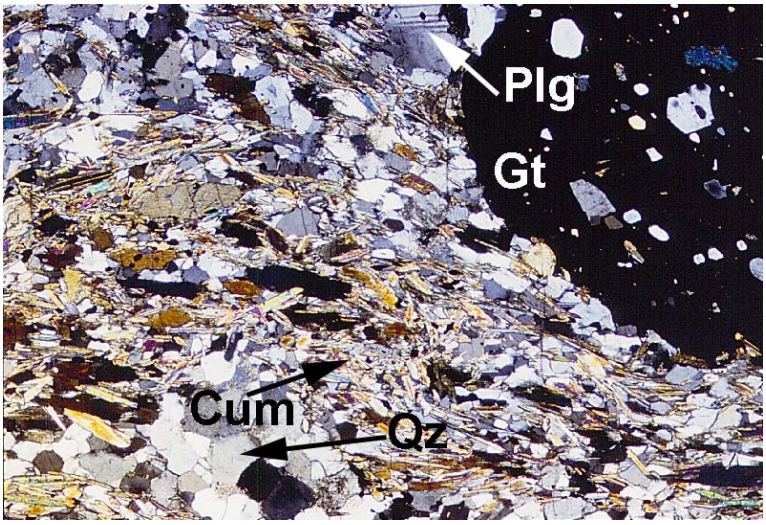

Figure 9. Photomicrograph showing garnet amphibolite in cross-polarized light. This photo shows a matrix of cummingtonite (Cum), plagioclase (Plg), and quartz (Qz) surrounding a large garnet (Gt) porphyroblast. View is 7 mm across the long dimension of the slide.

foliation, but does not exhibit the migmatitic texture present in rocks to the south. Weathered surfaces are generally slightly pink to orange. Although the unit commonly has the same four primary minerals as the migmatitic gneiss (K-feldspar, quartz, plagioclase, and biotite), the latter unit is much finer grained and darker in color due to abundance of biotite. The granite generally forms steep exposures in mountains and cliffs between the Tertiary volcanic rocks to the east and the Quaternary sediments to the west. It also forms inselbergs of moderate relief (30-100 m) in Quaternary sediments.

The Paleoproterozoic granite is intruded by narrow (~1 m) veins and dikes of pegmatite. It is also intruded in some areas by dikes of the Mesoproterozoic granite. The granite contains xenoliths of the migmatitic gneiss near its southern contact with that unit.

Microscopic Description

Minerals that comprise this unit are mainly K-feldspar, quartz, plagioclase, and biotite, and other minerals present include small amounts of sericite, and muscovite (probably retrograde), ilmenite, and sphene. Samples usually have a granoblastic texture, and contain a foliation defined by biotite. Feldspar locally occurs as phenocrysts and/or porphyroclasts. Although a foliation is generally present, this unit does not show any sense of shear (Figure 10).

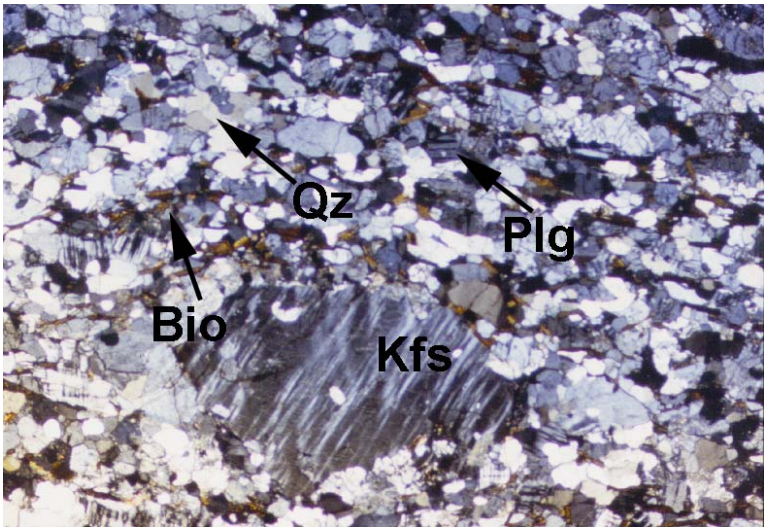

Figure 10. Photomicrograph showing Paleoproterozoic granite in cross-polarized light. The preferred orientation of minerals in this photo defines a foliation, but no shear sense is evident. Note lack of conspicuous asymmetry. This is an X:Z section and was cut from a sample from a mylonite zone, however, matrix quartz is completely recrystallized. Note the large K-feldspar (Kfs) porphyroclast in the center of the photo that is mantled by recrystallized grains as evidence for high temperature deformation (>450^{o}C). Other minerals are quartz (Qz), plagioclase (Plg), and biotite (Bio). View is 7 mm across the long dimension of the slide.

Interpretation

The predominance of K-feldspar and quartz and the presence of phenocrysts and xenoliths indicate that this unit is a deformed granite. The prominent foliation suggests that this unit has been subjected to high strains, while the lack of shear sense indicators suggests that the unit is not sheared or part of a shear zone.

Paleoproterozoic granite, undifferentiated (Xgu)

Macroscopic Descriptions and Field Relations

This unit is exposed in only one long narrow area in the northern part of the study area. It was separated out as a distinct map unit because it contains granitic rocks of many different textures and does not resemble any of the other granitic units. It is inferred to be Paleoproterozoic in age because many outcrops within this unit contain a metamorphic foliation and none are megacrystic indicating that they are not part of the Mesoproterozoic granite unit.

Paleoproterozoic Orthogneiss (Xog)

Macroscopic Descriptions and Field Relations

This unit consists of granitic gneiss exposed adjacent to the metasedimentary schist unit. It crops out north of Walnut Creek and south of Shingle Canyon. The dominant minerals in this unit are K-feldspar, quartz, and plagioclase, with a small

percentage of biotite. Hornblende is locally but not commonly present. Figure 11 shows a field photograph of a typical orthogneiss outcrop.

The orthogneiss unit is exposed as resistant cliffs and peaks in the same setting as that mentioned for the metasedimentary schist unit. Exposures of the orthogneiss are elongate as it contains a strong foliation and a locally developed lineation. Macroscopic shear sense indicators are present in some mylonite zones.

This unit is similar in mineralogy to the Paleoproterozoic granite unit, but is generally coarser grained and more gray and white. This unit contains dikes, veins, and other elongate bodies of pegmatite. The veins are generally much coarser-grained and more felsic than the orthogneiss unit rocks. Contacts with the metasedimentary schist unit are sharp and parallel to foliation in both units.

Microscopic Descriptions

K-feldspar is the most common mineral in the orthogneiss unit, followed by quartz, plagioclase, and biotite. Other minerals such as sericite, ilmenite, and zircon are present in very small quantities in some samples. K-feldspar occurs mostly as small recrystallized grains between larger K-feldspar phenocrysts and plagioclase. Quartz commonly occurs in narrow, elongate ribbons of large interlocking recrystallized grains. Plagioclase is present in each sample, but in lesser quantities than K-feldspar or quartz. It occurs as large isolated phenocrysts, commonly with albite twinning. Biotite is present in each sample, occurring as small flakes that define the foliation. It makes up less than 2% of any sample.

Figure 11. Field photograph showing Paleoproterozoic orthogneiss in outcrop. The orthogneiss is exposed here as a fine-to-medium grained granitic gneiss with strong subvertical foliation. Note that this outcrop contains two separate foliations (discussed in Chapter 3), each marked by a writing instrument. View is straight down at a horizontal surface. Pencil and pen for scale are each 15 cm long.

Rocks in the orthogneiss unit do not show strong shear sense indicators in thin section, but some mylonitic samples show a striped gneiss texture. Foliation is defined by this texture, ribbons of quartz, and aligned biotite grains.

Geochronology and Interpretation

A preliminary crystallization age of 1717 Ma was obtained for this unit based on five zircon grains using the U-Pb zircon dating technique (K. Chamberlain, personal communication, 2003). The sample for dating was taken from the northernmost outcrop of this unit in the study area. The sample outcrop contains the northeast-striking foliation, but is near areas of both north- and northwest-striking fabrics (discussed in Chapter 3).

The abundance of K-feldspar in this unit supports the inference that it is an orthogneiss rather than a high-grade paragneiss. The strong foliation and scattered mylonite zones suggest this unit has undergone a similar amount of strain to the metasedimentary schist unit. As mentioned in the metasedimentary schist rock description, that unit appears to contain veins of the orthogneiss unit, and therefore the orthogneiss is interpreted to be younger than the metasedimentary schist.

Although there are physical differences between this unit and the Paleoproterozoic granite unit, it is possible that they are related. They could represent different parts of the same intrusion. However, because of differences in texture and color, I chose to distinguish them as two separate map units in this study.

Unmetamorphosed Units

Mesoproterozoic Granite (Ygr)

Macroscopic Description and Field Relations

This granite is exposed in the northern part of the field area, generally west of the Paleoproterozoic granite and migmatitic gneiss units. The Mesoproterozoic granite is megacrystic with a local magmatic foliation defined by aligned euhedral K-feldspar phenocrysts, but is apparently not metamorphosed. It has been named the Holy Moses granite and is part of the continent-wide belt of ~1.4 Ga A-type granites (Anderson and Bender, 1989). The magmatic foliation was measured in a few locations and is subparallel to the foliation in nearby outcrops of migmatitic gneiss and Paleoproterozoic granite.

The megacrystic granite forms inselbergs (<100 m high) of large boulders and slopes of larger ridges where it occurs as rounded masses of outcrop and large boulders. Due to the fact that it is commonly exposed as out-of-place boulders, contacts between this unit and migmatitic gneiss or Paleoproterozoic granite are seldom found. At one such contact, magmatic foliation in this unit was concordant with the metamorphic foliation in the Paleoproterozoic granite and no emplacement-related structures were found. No thin sections of this unit were made.

Interpretation

Dikes of this unit have been observed to cross cut the foliation in other Proterozoic units. This observation, and the fact that the Mesoproterozoic granite lacks a foliation, indicates that this unit is younger than the other Proterozoic units. The only geochronological data on this granite is an old Rb/Sr age of 1.34 Ga (Kessler, 1976, reported in Bickford and Anderson, 1993).

Tertiary Volcanic Rocks (Tv)

Macroscopic Description and Field Relations

The eastern portion of the study area is entirely covered by Tertiary volcanic rocks. These rocks typically occupy the higher elevations of the study area, but are also in contact with the Proterozoic rocks at lower elevations. Rocks of this unit are typically basalt flows with minor rhyolite flows in some areas. In some areas a rhyolitic tuff common to much of western Arizona and southeastern California, the 18.5 Ma (Nielson et al., 1990) Peach Springs tuff, is present. Areas of questionable outcrop or mixed outcrop and volcanic colluvium are included in this unit on the map. The basalt flows of this unit form prominent ridge tops in some areas and reveal a regional tilt of only a few degrees.

Quaternary Older Alluvium and Colluvium (Qoa)

Macroscopic Description and Field Relations

Older alluvium and colluvium represents alluvium and colluvium consisting of sand and gravel to boulder-size sediments derived from all above units. This unit is found in inactive stream channels, washes, and colluvial deposits and includes alluvial fan materials and terrace materials. It also includes the mixed unconsolidated sediments of the Sacramento Valley.

Quaternary Alluvium (Qal)

Macroscopic Description and Field Relations

This unit is restricted to active stream channels and washes. This unit typically consists of sands and gravels consisting of the same materials as the older alluvium and colluvium unit.

CHAPTER 3: STRUCTURAL GEOLOGY

Regional Deformation in Northwestern Arizona

Paleoproterozoic rocks in northwestern Arizona are dominated by two metamorphic fabrics that have been associated with two regional deformational episodes, conventionally referred to as D_1 and D_2 in Arizona. In the North Virgin Mountains of southern Nevada, however, a fabric related to a deformational period temporally intermediate between the previously defined D_1 and D_2 events has recently been recognized (Quigley et al., 2002). Similar structures, discussed in detail below, have been documented in this study. For this reason, I propose a refined deformational chronology for central and northwestern Arizona in which D_1 is equivalent to the conventionally recognized D_1, D_2 is the newly recognized fabric in the northern Hualapai Mountains and North Virgin Mountains, and D_3 is equivalent to the formerly designated D_2 (Table 1)**.** This new terminology is used throughout this thesis.

The earliest fabric in central and northwest Arizona is associated with an enigmatic deformational event referred to regionally as D_1. The age of this event has been bracketed between 1740 and 1721 Ma in the nearby Cerbat Mountains (Duebendorfer et al., 2001a) and between 1740 and 1735 Ma in central Arizona (Karlstrom and Bowring, 1991). The S_1 foliation strikes north to northwest in northwestern Arizona and dips variably, from gently to steeply to the southwest and northeast. The tectonic significance of this early deformational episode is poorly understood. Some workers have viewed D_1 and D_3 (discussed below) as part of a protracted event related to the accretion of tectonic blocks to the growing North

Deformational Event	Duebendorfer et al., 2001a	Quigley et al., 2002	This study
Northwest-striking shallow-to-moderately-dipping foliation	D_1 (pre-1.72 Ga)	D_1	D_1 (pre-1.717 Ga)
North-striking foliation and fold axes	Not Recognized	D_2	D_2 (post-1.717 Ga)
Northeast-striking steeply-dipping foliation that reorients and overprints previous fabrics	D_2 (1.7-1.68 Ga)	D_3	D_3

Table 1. Table comparing the terminology used in different studies for the Paleoproterozoic deformational events of northwestern Arizona and southern Nevada.

American continental nucleus (e.g., Karlstrom and Bowring, 1988). Others have proposed that it represents the joining of the Mojave and Yavapai provinces prior to their accretion to the southern margin of Laurentia (Wooden and DeWitt, 1991; Duebendorfer et al., 2001a). Throughout northwestern and central Arizona this northwest-striking foliation has been reactivated and/or reoriented by a later northeast-striking fabric (S_3, see below) and in some areas has been completely overprinted by the later fabric.

Structures and fabrics assigned to the newly recognized D_2 event in the northern Hualapai Mountains overprint S_1 fabrics and are reoriented and reactivated by D_3 fabric. D_2 structures include mesoscopic folds and, possibly, significant reorientation of the S_1 foliation. Little has been published about the possibility of such a fabric existing elsewhere, but as discussed below, fabric of this orientation may have been documented in the northern Hualapai Mountains.

The dominant fabric in the study area and throughout much of the southwest United States is referred to here as S_3 (Karlstrom and Bowring, 1988). In the Cerbat Mountains, the D_3 event is bracketed between 1721 and 1682 Ma (Duebendorfer et al., 2001a). The S_3 foliation strikes northeast and dips steeply to subvertically. It is generally accepted among workers in the Proterozoic geology of the southwestern United States that this fabric represents the Yavapai orogeny (ca. 1700-1680 Ma) in Arizona and Colorado and the Ivanpah orogeny (ca. 1710-1690 Ma) in southern California (Wooden and Miller, 1990), and that these orogenies represent the accretion of the Mojave and Yavapai provinces to the southern margin of Laurentia (Karlstrom and Bowring, 1988; Anderson et al., 1993; Karlstrom et al., 1993; Duebendorfer et al., 2001a). There has been, however, some speculation about whether the Mojave and Yavapai provinces were

joined prior to the Yavapai/Ivanpah orogenies or whether multiple deformational events represent the piecemeal accretion of small terranes over as many as 60 m.y. (Albin and Karlstrom, 1991; Duebendorfer et al., 2001a).

Paleoproterozoic rocks in northwestern Arizona were intruded by ca. 1.4 Ga granitic plutons as part of a continent-wide magmatic event, the tectonic setting of which is controversial (e.g., Anderson, 1983; Windley, 1993; Nyman et al., 1994). Deformation associated with these intrusions is very localized or nonexistent (e.g., Ferguson, 2002, for the Hualapai Mountains; discussed in Chapter 1). No evidence exists for deformation in northwestern Arizona between 1.4 Ga and the latest Cretaceous to early Tertiary Laramide orogeny. At that time broad uplifts exposed the Proterozoic basement rocks and the overlying Phanerozoic cover was eroded away (Young, 1979; discussed in Chapter 1). During the period of middle to late Tertiary Basin and Range extension, Proterozoic rocks in northwestern Arizona were faulted and tilted, but large areas appear to have retained their original orientations, as fabrics are similar to those found on the undeformed Colorado Plateau (discussed further in Chapter 1).

Deformation in the Northern Hualapai Mountains

Introduction

The northern Hualapai Mountains contain both the northwest-striking (S_1) and northeast-striking (S_3) fabrics that have been attributed to the two major Paleoproterozoic deformational events elsewhere in Arizona. In addition, they contain a fabric (S_2) temporally intermediate between the development of the northwest- and northeast-striking fabrics. The study area contains no penetrative fabrics younger than the

northeast-striking S_3 foliation. A granitic pluton (Holy Moses granite) related to the widespread 1.4 Ga intrusions in the southwestern United States is present in the study area, but there is no evidence for deformation of this pluton. Locally, pre-1.4 Ga fabrics, particularly the 1.7 Ga S_3 foliation, appears to have controlled emplacement of these plutons. Tertiary faults are present in the study area, but Tertiary deformation and volcanic rocks are not the focus of this study and they do not appear to have significantly modified the orientations of the Proterozoic rocks. For example, fabric orientations in the Hualapai Mountains closely match orientations in rocks of similar age on the Colorado Plateau that have not been appreciably deformed since the Proterozoic (Ilg et al., 1996).

Evidence for Polyphase Deformation

There has been discussion over the past few decades about whether the two primary Paleoproterozoic fabrics in Arizona are the product of one progressive deformational episode (e.g., Albin and Karlstrom, 1991) or separate orogenic events (e.g., Wooden and DeWitt, 1991; Duebendorfer et al., 2001a). However, the number of deformations an area has undergone cannot be deduced from fabric orientations alone. The question of whether an area has experienced polyphase or progressive deformation can be addressed by establishing whether fabrics in the area can be separated into multiple generations. Separate fabric generations can be identified by a difference in synkinematic mineral assemblages between fabrics and/or overprinting and cross-cutting relationships.

The northern Hualapai Mountains contain at least three temporally distinct metamorphic fabrics, the relative timings of which are determined by cross-cutting and

overprinting relations. Map foliation patterns show complex geometries that strongly suggest reorientation or overprinting of earlier fabrics by later fabrics. Although there is no location in the study area that exhibits clear-cut fold interference patterns suggestive of multiple phases of folding (e.g., F_1, F_2, F_3), it is unlikely that one progressive deformational episode could produce the strong variability in fabric orientations present in the northern Hualapai Mountains.

Paleoproterozoic Deformation

Domains

The study area can be divided into areas of dominantly northwest-striking and northeast-striking foliation, and therefore I identified four structural domains (Plate 2). Domain 1 is the most northerly part of the study area and contains Paleoproterozoic granite with generally northwest-striking fabric. Domain 2 encompasses the majority of the study area and contains most of the northeast-striking fabric in the area. Domain 3 is near the center of the study area and contains metasedimentary schist and orthogneiss with northwest- and north-striking fabrics and small areas of other fabric orientations that are reoriented into a northeast-striking foliation southeast of the domain boundary. Domain 4 is in the southern and southeastern part of the study area and is divided into two parts (Domains 4a and 4b) because it contains an area of primarily northwest-striking fabric (Domain 4a) and an area containing northeast-striking fabric (Domain 4b), separated by a small area of north-striking fabric. Domain 4a is separated from Domain 4b by mesoscopic folds with north-trending axes (discussed below). Domain 4b contains

rocks farther east in Walnut Canyon and fabric in this area is variable in orientation with zones of both S_1 and S_3 fabrics present as well as folds at various scales.

Northwest-striking Foliation (dominantly related to S_1)

The northern Hualapai Mountains contain several areas of northwest-striking foliation that have not been overprinted by later deformational events. This foliation typically dips moderately to steeply to the southwest and northeast, and due to its similarity in orientation to the documented D_1 fabric (i.e., pre-1720 Ma) in the Cerbat Mountains, is correlated with D_1.

The largest area of northwest-striking fabric is in Domain 1 (Plate 2). Along the Domain 1/Domain 2 boundary and within the Paleoproterozoic granite rock unit (Plate 1), the fabric undergoes a complete reorientation from northwest striking to northeast striking (i.e., into S_3). Between the two distinct fabric domains is a map-scale fold that indicates that the northeast-striking fabric reoriented rather than overprinted the northwest-striking foliation in that location. There is no discrete cross-cutting relationship between S_1 and S_3 along the Domain 1/Domain 2 boundary. The two distinct foliation orientations within the same rock unit may be evidence that the northwest-striking foliation was undergoing reorientation to a northeast direction at the time northeast-striking shear zones, such as the Gneiss Canyon shear zone in the Grand Canyon, were active.

In the Paleoproterozoic granite unit, aligned biotite and quartz grains define the foliation. In the migmatitic gneiss unit, alignment of minerals and compositional banding

define the foliation, resulting in striped migmatitic rocks (Figure 4). Texturally, the metasedimentary schist varies from extremely schistose, where micaceous (Figure 12), to more gneissic (i.e., compositional banding) where more feldspar and quartz is present (Figure 13). Although mica content varies, aligned biotite grains are the best indicators of foliation throughout the unit.

North-striking Fabrics (Dominantly related to D_2 deformation [?])

At least two locations in the study area contain a local north- to northwest-striking fabric that postdates the northwest-striking foliation but predates the northeast-striking foliation (Figure 14). This temporally intermediate fabric could be equivalent to or related to fabrics of the same orientation in the North Virgin Mountains of southern Nevada (Quigley et al., 2002). In the southernmost part of the study area, at station 56 (Plate 3), a series of mesoscopic cylindrical folds with north-trending fold axes is present in an area of transition between domains of northwest-striking (Domain 4a) and northeast-striking (Domain 4b) foliations (Rhys-Evans, 2003). The mesoscopic cylindrical folds are also nearby in both domains. The angle between the hinge of the folds and strike of foliation is the same in both domains, approximately 50^{o}. These similar relations indicate that the folds overprinted the earlier northwest-striking foliation (D_1), and then were rotated ~90^{o} during D_3, as the northeast-striking foliation was formed (Figure 15). The mesoscopic folds appear to be the only evidence of this deformational event in the southern part of the study area. There are other small areas of north- and northwest-striking fabric, but overprinting relations that suggest a temporally

Figure 12. Field photograph showing schistose texture in metasedimentary schist. Dark streaks are micaceous areas consisting primarily of biotite. View cross-sectional and perpendicular to foliation plane. Hammer for scale (40 cm long).

Figure 13. Field photograph showing gneissic texture in metasedimentary schist. Quartzofeldspathic veins cut the gneissic fabric and therefore postdate it. Note shear band in center of photo. View is map view. Hammer for scale (40 cm long).

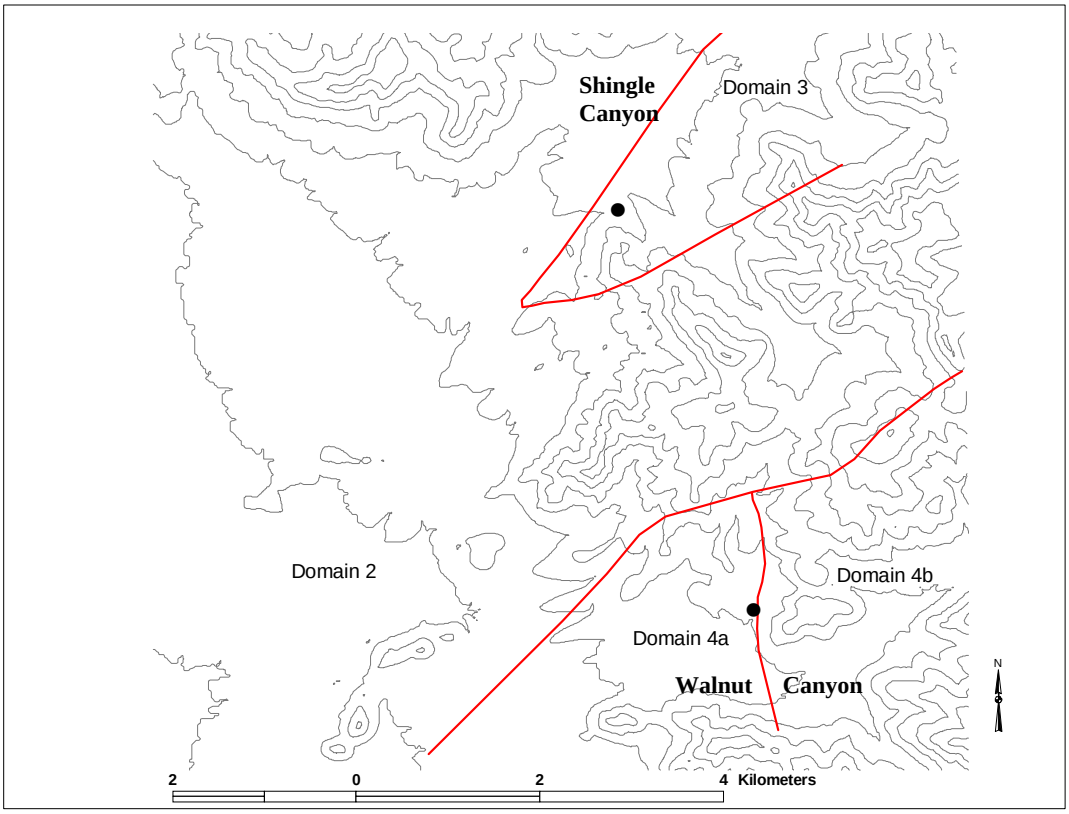

Figure 14. Figure showing localities containing S_2 fabric, as represented by large dots. Contour interval is 300 feet. This area is shown on Plate 2.

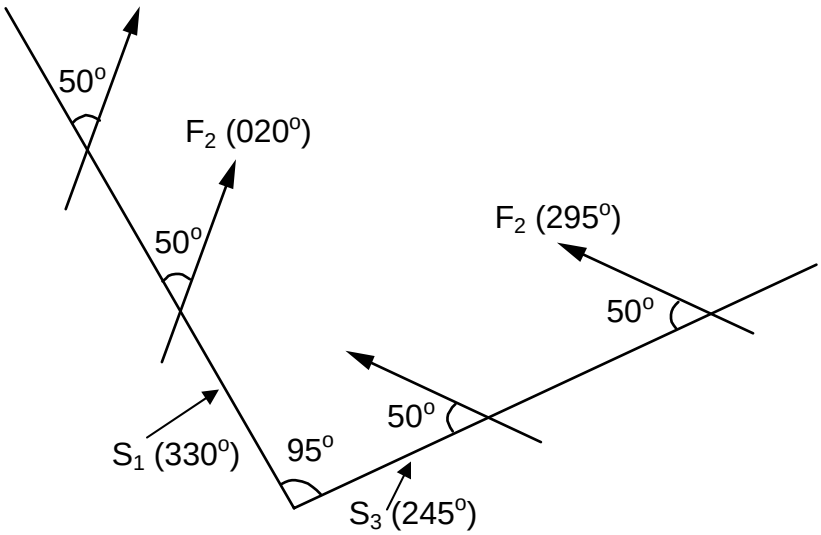

Figure 15. Schematic diagram from field sketch showing three separate fabrics at station 56. If S_3 is back-rotated to the orientation of S_1, all F_2 folds trend between 020° and 030°. Arrows represent F_2 fold axes. Diagram is oriented with north at the top of the page and diagram is approximately 10 m wide.

intermediate fabric such as those shown in Figure 15 do not occur at any other locations. These other smaller areas of north- and northwest-striking fabric are commonly found in the hinge areas of map-scale folds.

In an area just south of Shingle Canyon within Domain 3, at station 60 (Plate 3), a significant area of northwest strikes associated with D_1 and an area with north strikes associated with D_2 occurs in the orthogneiss unit. This unit yielded a preliminary U/Pb zircon date of 1717 Ma (K. Chamberlain, personal communication, 2003) only a few hundred meters away from station 60. Therefore, at least at this location, and possibly throughout the northern Hualapai Mountains, the northwest- and north-striking fabrics should post-date D_1 (1740-1721 Ma) as defined in the Cerbat Mountains and elsewhere in Arizona (Duebendorfer et al., 2001a). However, the margin of error on the date of 1717 Ma has not yet been calculated and if reasonable margin of error (2-3 Ma) is assumed for both the 1717 Ma date and the 1721 Ma date in the Cerbat Mountains, the error bars should overlap. In such a situation the orthogneiss in the northern Hualapai Mountains may have intruded coevally with or prior to the D_1 event.

Northeast-striking Foliation (Dominantly assigned to D_3)

A northeast-striking, steeply dipping foliation that reorients and overprints the north- and northwest-striking fabrics is best developed in Domain 2. In the northern part of the study area, the northwest-striking foliation is folded into the northeast-striking foliation at the map scale. There is no evidence near this fold for an overprinting relationship (i.e., reorienting of minerals within a fabric) between S_1 and S_3. In Walnut

Canyon, a few kilometers southeast of the study area, the northeast-striking foliation reorients the northwest-striking foliation, producing anomalous lineation trends (Duebendorfer, 2003). Field evidence was also found for the local overprinting of S_1 by S_3 (Figures 16, 17). Foliation and lineation are defined in the same way as in the northwest-striking foliation, discussed above, implying that D_3 did not produce a new pervasive fabric (e.g., defined by new mineral growth), but only locally overprinted the earlier fabrics. In most areas, D_3 reoriented the north- and northwest-striking fabrics.

Mylonitic Foliation

Mylonite zones are abundant in the metasedimentary schist and migmatitic gneiss units and are also present in the orthogneiss unit (Figure 18). They are less common in northwest-striking areas than northeast-striking areas, although there appears to be no difference in character (i.e., degree of grain-size reduction, metamorphic grade) between mylonite fabrics in areas of either deformational fabric. The mylonite zones are typically 10 cm-10 m wide, range from tens of meters to a few hundred meters in length, and are consistently oriented concordant to the local foliation. As shown in Figure 10, mylonites contain K-feldspar grains with core and mantle structures, indicating deformation by recrystallization. Therefore, the temperature of deformation must have exceeded 450^{o}C.

Most mylonite zones do not contain a lineation or obvious kinematic indicators and therefore they appear to have accommodated flattening strains, as they contain symmetrical porphyroclasts (Figure 10). However, some of the zones contain evidence

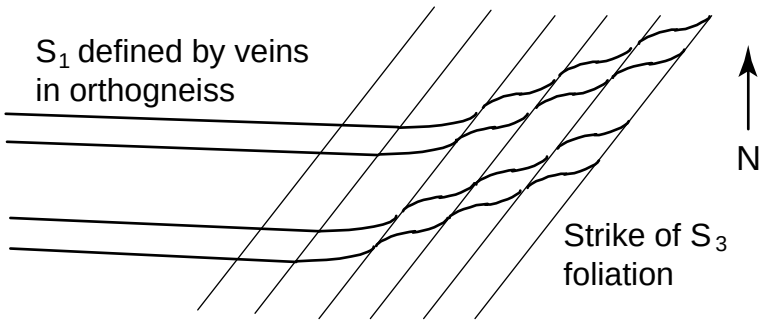

Figure 16. Schematic diagram showing overprinting relation between S_1 and S_3. Map view of outcrop approximately 2 meters across.

Figure 17. Field photograph showing S_1 and S_3 fabrics in orthogneiss. The Sharpie pen on the left is parallel to S_1 and the pencil on the right is parallel to S_3. The overprinting relationship between the two fabrics is diagrammed in Figure 18. View is straight down on a horizontal surface. The top of the photo is northeast, with the photo edge approximately parallel to the strike of S_3. The pen and pencil for scale are each 15 cm long.

Figure 18. Field photograph showing cross-sectional view of outcrop-scale mylonite zone in metasedimentary schist. View to northeast (065^{o}). Hammer placed in vertical joint (lower center of photo) is 40 cm long.

for simple shear and 21 shear sense indicators were found in the study area. Kinematic indicators in the study area were documented only within mylonites zones.

Shear sense in lineated mylonite is generally indicated by asymmetrical porphyroclasts. Of the 21 kinematic indicators found in the study area, most showed weak shear sense (i.e., some kinematic interpretations are based on poorly developed asymmetrical porphyroclasts and some kinematic interpretations are based on the majority shear sense direction when multiple porphyroblasts show more than one direction of shear sense). Only two kinematic indicators were found in the northwest-striking domains (4a and 4b in the southeast part of the study area, see Plate 2) and both of those show northeast-side up shear sense (Table A-1, in appendix). Nineteen kinematic indicators are located in northeast-striking zones and 13 of those show northwest-side-up shear sense. Six show southeast-side-up shear sense (Table A-1, in appendix). Kinematic indicators showing northwest-side-up shear sense are best developed in the southern part of Domain 2, while those showing southeast-side-up shear sense are best developed in the northern part of Domain 2 (Figure 19). Of the 21 kinematic indicators, 12 indicate reverse-sense motion, three indicate vertical motion, and six indicate normal-sense motion (Figure 19), however, five out of the six normal-sense indicators are on foliation planes dipping 80^{o} or more. Given that these five indicators are close to having a vertical sense of shear, it is clear that the dominant sense of motion on mylonite zones in the study area is reverse-sense on steeply-dipping and subvertical shear zones.

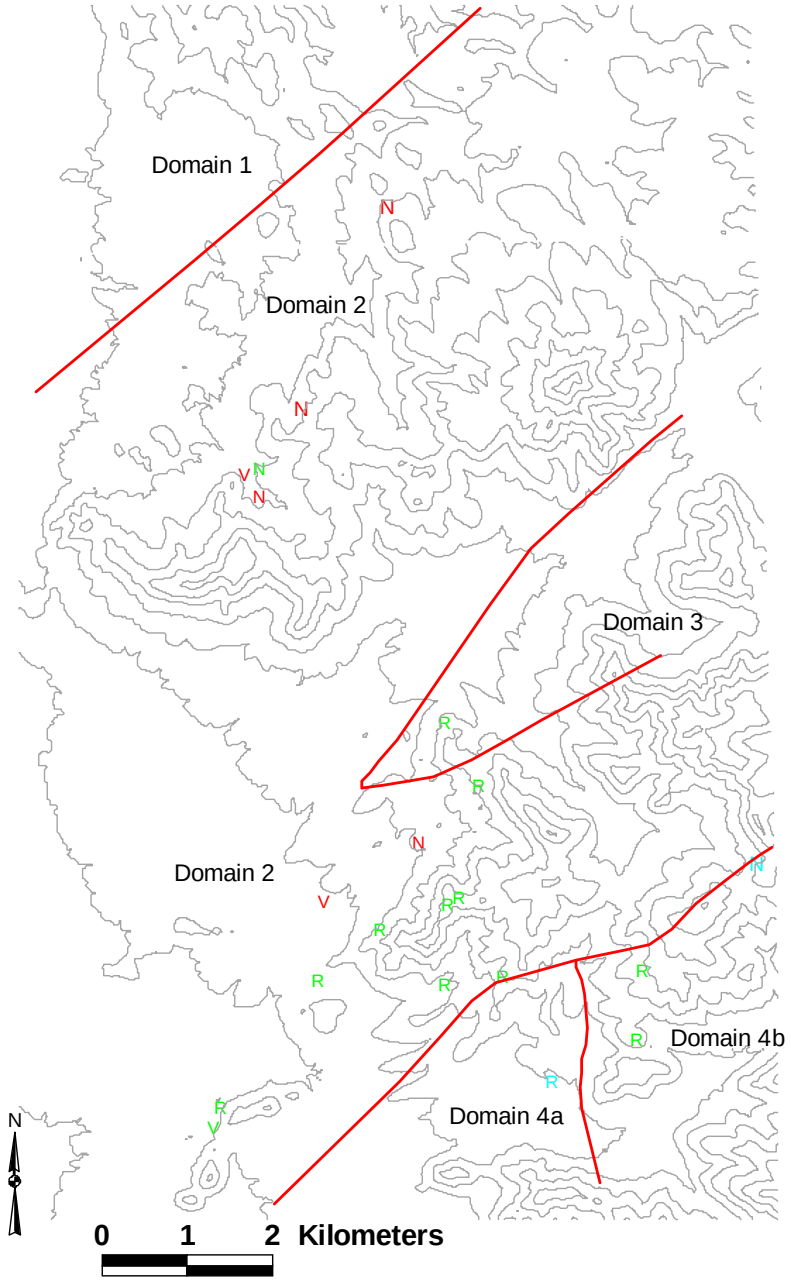

Figure 19. Map of the study area showing locations of kinematic indicators and the shear sense of each indicator. Green markers indicate northwest-side-up shear sense, red markers indicate southeast-side-up, and blue markers indicate northeast-side-up. An "N" symbol indicates normal-sense movement, a "V" symbol indicates vertical movement, and an "R" indicates reverse-sense movement. Contour interval is 300 feet.

Folds

Folds at all scales are present in the study area and the orientation and geometry of folds do not appear to be related to the structural domains in which they occur. Therefore, this discussion is separate from the discussions of deformational fabrics. Folds appear to be preferentially developed in metasedimentary units rather than igneous units, although this may be due to a lack of markers in igneous rocks. One map-scale fold with a steeply plunging hinge line is present at the boundary of structural Domains 1 and 2 (see Plate 2). This fold represents a transition between the northwest- and northeast-striking fabrics. Other macroscopic folds occur completely within the northeast-striking fabric, such as in the valley south of station 21 and at station 3 (Plate 3). The tectonic significance of these folds is unknown.

The D_1 fabric in the Cerbat Mountains has been reported to consist of recumbent folds with highly attenuated limbs that have been detached from their hinges, and rootless intrafolial folds (Orr, 1997; Jones, 1998; Duebendorfer et al., 2001a). No rootless intrafolial folds (i.e., F_1) within the northwest-striking foliation were recognized, indicating that strong transposition occurred during the D_1 event to transpose the hinges of any F_1 folds that may have existed. Another possible explanation for the lack of F_1 fold hinges is that they could have been transposed during northwest-southeast contraction (D_3). Some outcrop-scale folds have been found in low D_3 strain zones and these probably represent incompletely transposed F_1 or F_2 folds (Figure 20). It appears that the high levels of strain recorded in these rocks have destroyed much of the evidence for folding and left mostly strongly transposed foliation and ptygmatic folds.

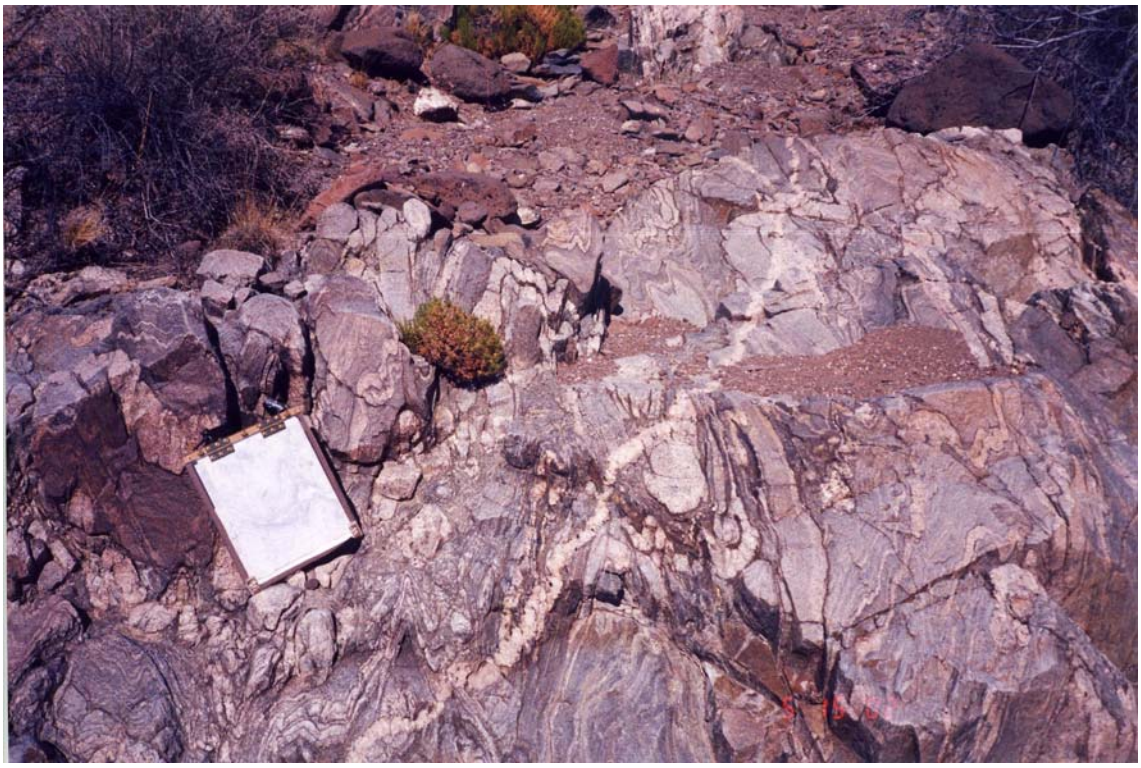

Figure 20. Field photograph showing transposition of S_1 and/or S_2 into S_3 in migmatitic gneiss. S_3 strikes nearly parallel to the view direction. Ptygmatic folding is present as well. Photo faces ENE (072^o) obliquely down at gently west-dipping surface. Map board is 25 cm wide.

Eighteen fold axes from outcrop-scale and smaller folds were measured, however, a stereonet plot of the fold axes does not reveal a strong preferred orientation except that most plotted within a weak northeast-southwest-trending girdle (Figure 21). The mesoscopic folds range from gentle to isoclinal in tightness and map-scale folds typically have larger interlimb angles, although this observation may be biased by the destruction of tighter fold hinges, making those folds unidentifiable (Table A-2 in appendix). There appears to be no correlation between fold tightness, hinge orientation, and shape and orientation of foliation (i.e., structural domain) with the exception of the mesoscopic cylindrical folds at station 56 that characterize D_2 in that area (Plate 3).

Lineation

Lineation in areas of all foliation orientations is defined by preferential grouping of minerals such as elongate quartz, feldspar, and biotite as viewed on the foliation plane (Figure 22). Lineations measured in the northwest-striking Domain 1 generally plunge down-dip on the local foliation. The lineation orientations in Domain 1 are tightly grouped and plunge steeply to the southwest (Figure 23) and because fabrics within Domain 1 are correlated with D_1, these southwest-plunging lineations are considered to be L_1 lineations. Lineation orientations on northwest-striking foliation planes in other domains are less consistent.

Lineations recorded in Domain 3 are grouped as north-trending, moderately plunging (Figure 23C), and may be rotated L_1 lineations. Possible rotation of L_1 lineations in an area not overprinted by S_3 further suggests the presence of the

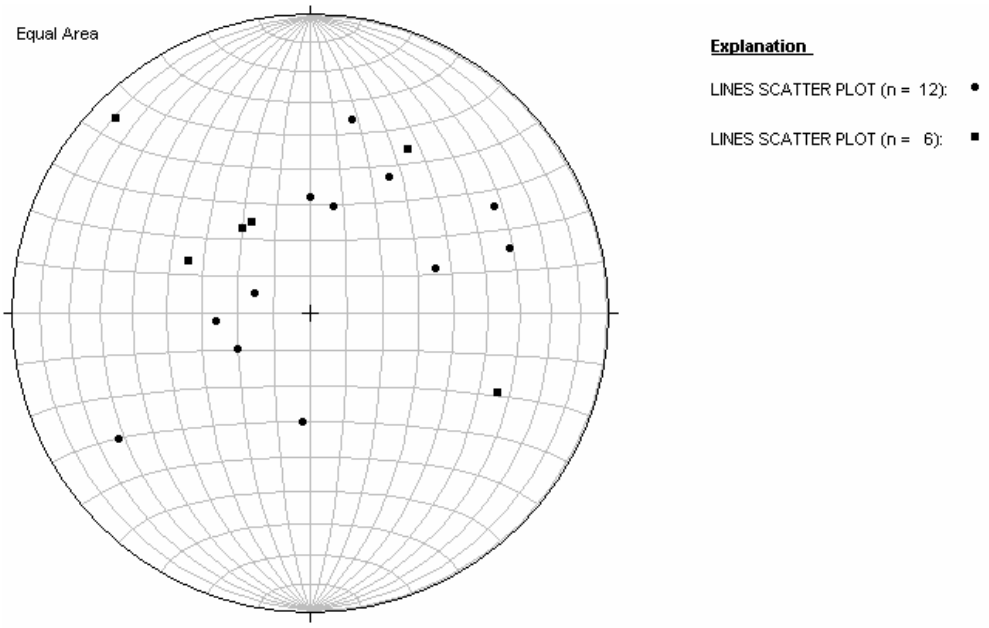

Figure 21. Lower hemisphere stereonet projection of mesoscopic and macroscopic fold axes. Measured hinge lines are represented by circles and constructed axes are represented by squares. Note that measured hinge lines appear to plot in a weak northeast-southwest-trending girdle and plunge moderately to steeply. Constructed fold axes plot within this loose girdle with few exceptions.

Figure 22. Photograph of hand sample showing lineations on foliation plane. Lineations are defined by light and dark streaks consisting of concentrations of quartz, feldspar, and biotite. This is a sample of orthogneiss. Similar lineations are preserved in other units. Sample measures 10 cm from left to right.

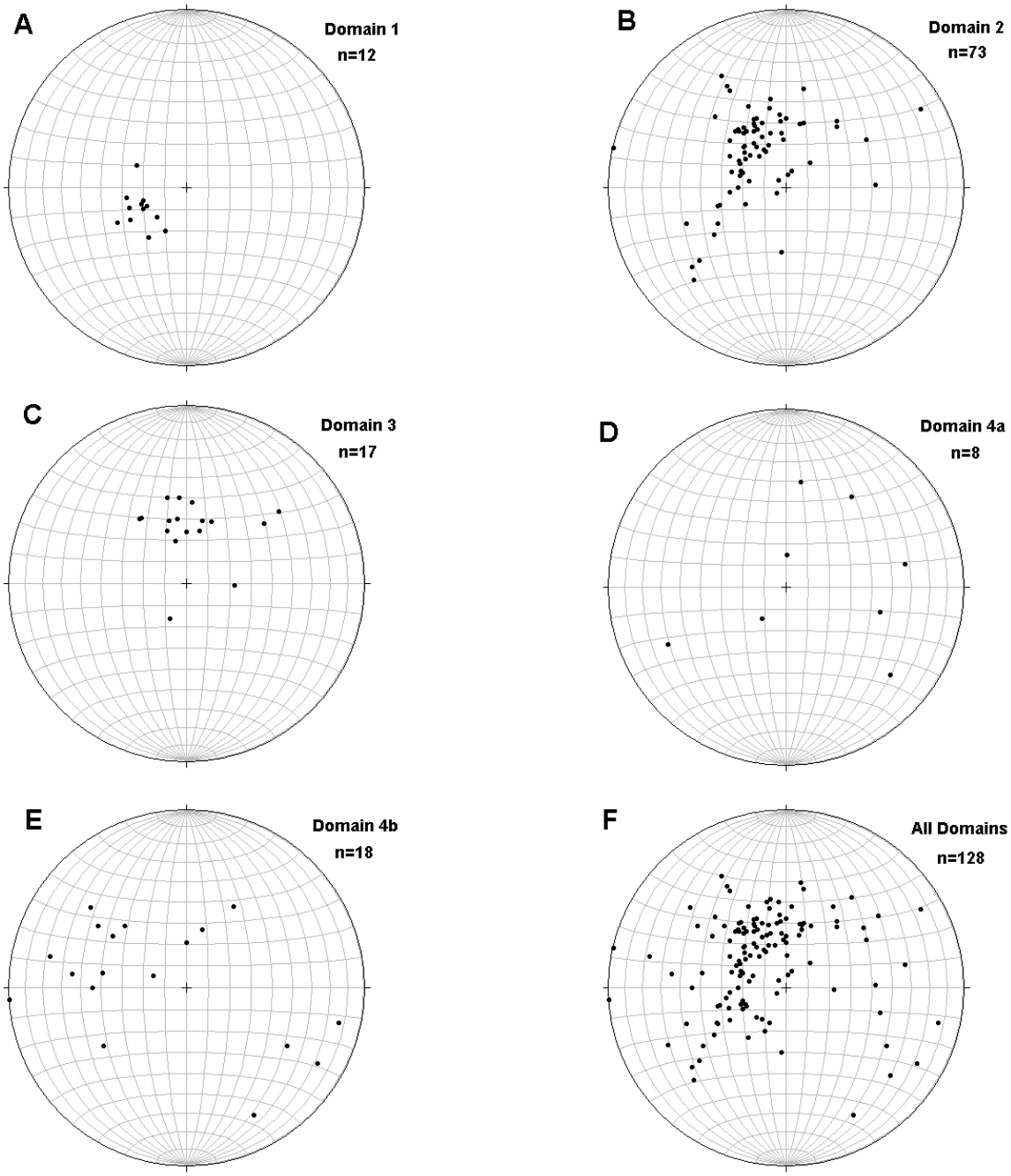

Figure 23. Lower hemisphere stereonet projections of lineations in the northern Hualapai Mountains. There is a separate projection for each domain, including a projection of lineations from all domains (F, lower right). Domain 1 lineations (A) are considered to be L_1 lineations and are associated with the NW-striking foliation (S_1). Domain 2 lineations (B) are associated with the NE-striking foliation (S_3). Domain 3 lineations (C) trend north and may be related to the N-trending D_2 fabric. Note considerable scatter in Domain 4a and 4b lineations (D and E).

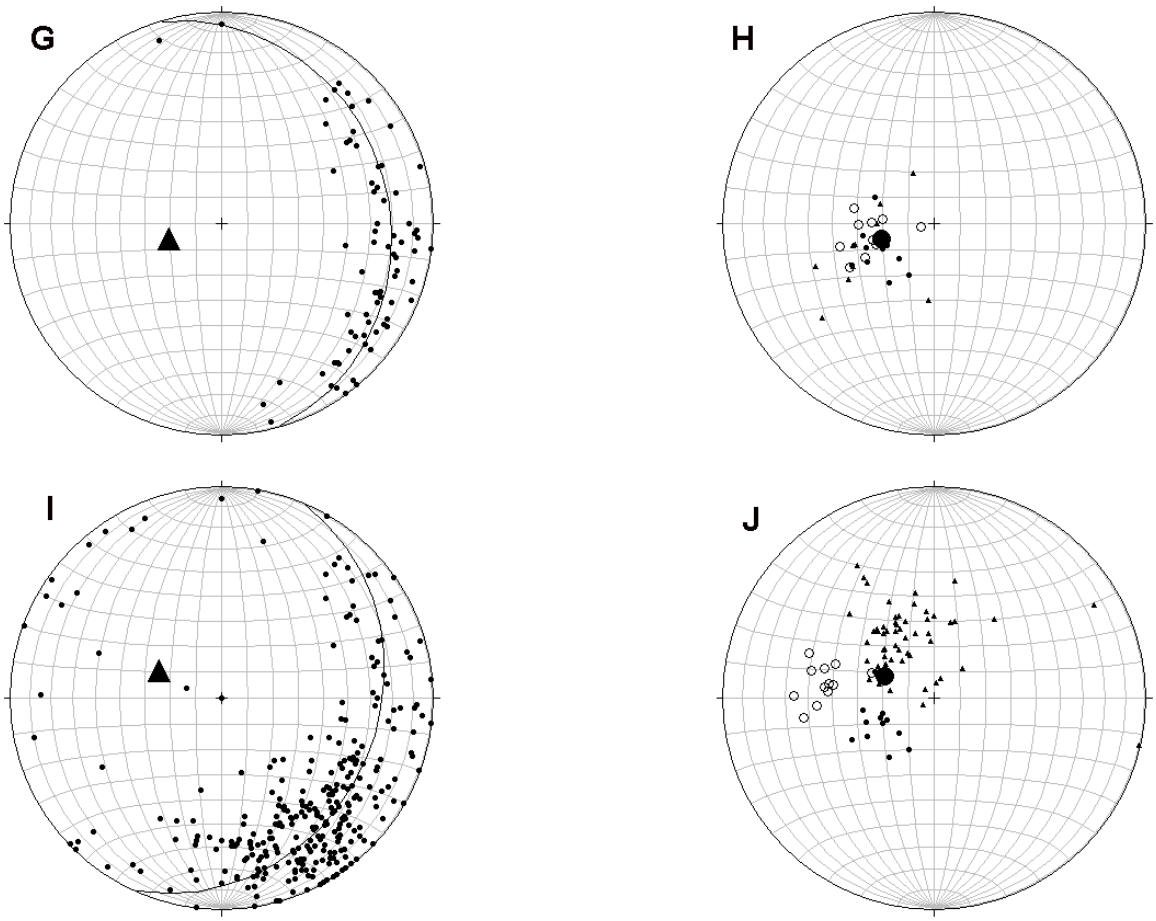

Figure 23 (continued). Figure 23G shows poles to foliations from Domain 1 and the north area of Domain 2, near the Domain 1/Domain 2 boundary. The triangle represents the best-fit fold axis between the Domain 1 and 2 foliations (fold axis: 69, 254). Figure 23H shows Domain 1 lineations (filled circles), the fold axis from Figure 23G (large filled circle), Domain 1 lineations rotated about the fold axis (magnitude: 85^{o} clockwise; hollow circles), and lineations from the north part of Domain 2 (filled triangles). Note that all three lineations sets have similar orientations. Figure 23I shows poles to foliations from Domain 1 and the south area of Domain 2. The triangle represents the best-fit fold axis between the Domain 1 and 2 foliations (fold axis: 64, 294). Figure 23J shows Domain 1 lineations (filled circles), the fold axis from Figure 23I (large filled circle), Domains 1 lineations rotated about the fold axis (magnitude: 85^{o} clockwise; hollow circles), and lineations from the south part of Domain 2 (filled triangles).

intermediate deformational event in Domain 3. Lineations measured in areas of northeast-striking foliation (primarily Domain 2) show a preference to plunge moderately to steeply northwest (Figure 23).

Because lineations found in areas of northwest- and northeast-striking fabric are defined in the same way, it is not possible to discern in hand sample or thin section whether the lineations are related to D_1, D_2, or D_3. Therefore, I have used a geometrical analysis to evaluate the possibility that L_1 lineations may have been rotated by a later deformation. Figure 23H shows a stereonet projection of lineations from Domain 1 rotated 85° clockwise (the approximate angle between the S_1 and S_2 foliations at the Domain 1/Domain 2 boundary) around the constructed axis of the fold between Domain 1 and Domain 2. This fold axis is subparallel to the lineations in Domain 1, however, so the rotation resulted in a minimal change in Domain 1 lineation orientation. It is important to note that lineations in the northern part of Domain 2, near the Domain 1/Domain 2 fold, are similar in orientation to Domain 1 lineations as well (Figure 23H). This relationship allows for the possibility that lineations found in Domain 2 are rotated L_1 lineations because the fold axis is subparallel to lineations from both domains, but also allows for the possibility that the lineations in both domains were acquired during or after the folding. It cannot be proven from the data presented here that the lineations in the northern part of Domain 2 are rotated L_1 lineations.

Figure 23J shows a stereonet projection of lineations from Domain 1 rotated 85° clockwise around the axis generated from using Domain 1 foliations and southern Domain 2 foliations as fold limbs. Lineations from southern Domain 2 are plotted as well, but do not plot near the rotated Domain 1 lineations (Figure 23J). This relationship

suggests that the lineations in the southern part of Domain 2 are not rotated L_1 lineations, and they may represent a generation of lineations associated with D_3.

Mesoproterozoic Deformation

The Mesoproterozoic granite is magmatically foliated in many exposures and the magmatic foliation is concordant with the metamorphic foliation in nearby Paleoproterozoic rocks everywhere the magmatic foliation is present. Contacts with Paleoproterozoic rocks reveal little about the nature of emplacement of the Mesoproterozoic granite, but the concordant magmatic and metamorphic foliations suggest that the existing pre-1.4 Ga fabrics (especially S_3) may have controlled emplacement of the Mesoproterozoic granite. There is no evidence that the 1.4 Ga intrusions deformed the Paleoproterozoic rocks of the study area.

Tertiary Deformation

Although the Proterozoic rocks are believed to be largely undeformed by Phanerozoic events, there is evidence in the study area for some Tertiary faulting. Basalt flows are noticeably offset in a few locations and two likely fault zones have been identified.

A small fault is present in Proterozoic rocks at station 50 (north of Shingle Canyon, in Griffith Wash) (Figure 24, Plate 3). The fault appears to separate two lithologies within the metasedimentary schist unit and trends 002^{o} as exposed on a flat erosion surface. The fault zone is narrow with only a few centimeters of gouge evident and no brittle kinematic indicators were observed. However, north of the station are

Figure 24. Field photograph showing a brittle fault cutting the metasedimentary schist unit at station 50. The photo faces a horizontal surface with east at the top of the photo. The GPS receiver for scale is approximately 15 cm long.

basalt flows that appear to be offset. Between the apparently offset flows is an area with brecciated basalt boulders in the talus. Because the fault trace from station 50 projects toward this brecciated area between basalt flows, I interpret the boulders to be fault breccia. This location is the only place in the study area where a Tertiary fault was observed cutting both Proterozoic and Tertiary rocks.

Another likely Tertiary fault zone is located to the south where a basalt flow is offset across a small valley (Figure 25, Plate 1). Fault offset was not measured, but based the field photograph offset is estimated at 50-100 m. However, in this location, no faults were found in Proterozoic rocks.

Figure 25. Field photograph showing offset basalt flow. The flow is visible on the left side of the photo as a horizontal outcrop line. The flow is visible on the right side of the photo as the ridgeline, which terminates near the drainage in the center of the photo. This drainage may have formed along a Tertiary fault trace.

CHAPTER 4: CONDITIONS OF METAMORPHISM

Introduction

The primary rock types in the study area are plutonic or psammitic, neither of which is sufficiently aluminous to produce the mineral assemblages required for the use of a geobarometer such as GASP. However, two locations in the study area do contain pelitic schist (stations 47 and 59, Plate 3) and samples were collected from each for geothermometry (garnet-biotite) and geobarometry (GASP). Both pelitic schist locations contained a primary mineral assemblage of K feldspar + quartz + biotite + plagioclase + garnet + sillimanite, with no discernible prograde muscovite. Polished thin sections were obtained and the electron microprobe was used to obtain the chemical data necessary for the analyses.

Unfortunately, the samples collected at station 47 could not be used for barometry because the plagioclase in those samples was nearly end-member albite and GASP requires a higher calcium content to be valid. The samples collected at station 59 contain anorthite values of 23-26% and are suitable for barometry.

Methods and results of geothermometry and geobarometry

The Cameca MBX electron microprobe at Northern Arizona University was used to analyze mineral compositions in the samples collected at station 59. Operating conditions of the microprobe were an accelerating voltage of 15 KeV, beam current of 10-25 nA, a spot size of 1 μm, and counting times of 30-33 seconds. Ferric iron was assumed to comprise 15% of the total iron in biotite. The geothermometer used was the

garnet-biotite thermometer of Holdaway (2000) and the geobarometer used was the GASP (garnet-aluminosilicate-plagioclase) barometer of Holdaway (2001). Traverses of 200 points each were analyzed on samples SC13A-A and SC13B and individual points were chosen for thermometry and barometry that appeared to be near the center of the garnet grain and were least likely to be retrograded. Seven points were chosen from the traverse on sample SC13A-A (points 100-106) and five points were chosen from the traverse on sample SC13B (points 282, 289, 301, 319, 323). Figure 26 shows photomicrographs of each sample and the paths of the traverses. Table 2 shows averaged chemical data for all points used for analysis. Figure 27 shows temperatures and compositions across each garnet profile.

Thermometry and barometry on sample SC13A-A yielded a temperature of 653^{o} C and a pressure of 5.2 kilobars (Figure 28A). Sample SC13B yielded a temperature of 661^{o} C and a pressure of 5.1 kilobars (Figure 28B). A sample collected from the northern Hualapai Mountains in an area just southeast of the study area yielded a temperature of 605^{o} C and a pressure of 5.4 kilobars and a sample collected several kilometers south of the study yielded a temperature of 630^{o} C and a pressure of 5.3 kilobars (Duebendorfer et al., 2001b).

The rocks in the study area plot somewhat higher in temperature on the KNAFMASH petrogenetic grid (Figure 29). In order to react out all prograde muscovite and create K-feldspar and sillimanite, the rocks must have reached nearly 700^{o} C (Figure 28). These deviations (40-50^{o} C) from the garnet-biotite thermometer's results are explained by diffusive retrogradation of the garnets all the way to their centers (note temperature profile for sample SC13A-A, Figure 27A), making it impossible to quantify

Garnet			Biotite			Plagioclase		
Sample	SC13AA	SC13B	Sample	SC13AA	SC13B	Sample	SC13AA	SC13B
MgO	2.931	3.865	Na2O	0.14	0.073	Na2O	8.886	8.502
Al2O3	20.921	21.374	MgO	6.787	8.019	MgO	0.002	0
SiO2	36.61	37.016	Al2O3	19.197	18.292	Al2O3	24.032	24.762
CaO	1.01	1.048	SiO2	34.08	34.386	SiO2	62.854	61.65
MnO	1.07	1.232	K2O	9.996	10.111	K2O	0.235	0.185
FeO	36.211	36.207	CaO	0.022	0.024	CaO	4.896	5.605
Total	98.753	100.742	TiO2	2.542	3.954	TiO2	0	0.001
SUM O	12	12	MnO	0.11	0.024	MnO	0	0
Mg	0.357	0.461	FeO	21.563	20.628	FeO	0.005	0.017
Al	2.015	2.015	Total	94.437	95.51	Total	100.911	100.722
Si	2.992	2.961	SUM O	11	11	SUM O	8	8
Ca	0.088	0.09	Na	0.021	0.011	Na	0.756	0.727
Mn	0.074	0.083	Mg	0.791	0.92	Mg	0	0
Fe2+	2.475	2.422	Al	1.769	1.66	Al	1.244	1.287
			Si	2.664	2.648	Si	2.76	2.718
			K	0.997	0.993	K	0.013	0.01
			Ca	0.002	0.002	Ca	0.23	0.265
			Ti	0.149	0.229	Ti	0	0
			Mn	0.007	0.002	Mn	0	0
			Fe2+	1.41	1.329	Fe2+	0	0.001

Table 2. Table showing averaged chemical data for each sample used in barometry and thermometry. Garnet data represent the average of all points used for analysis (7 points for SC13A-A, 5 points for SC13B). Biotite and plagioclase data represent the average of three points per mineral from each sample.

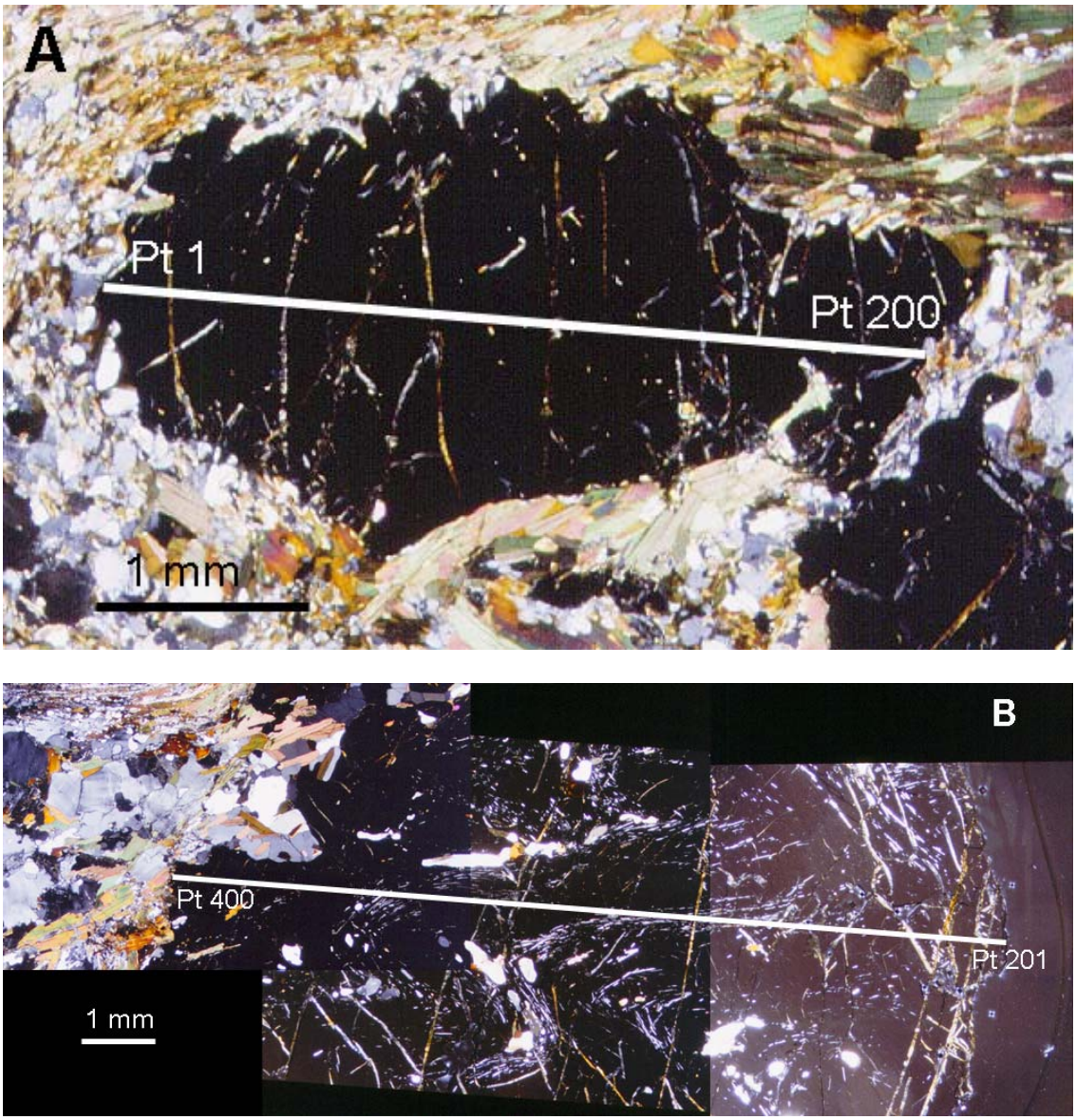

Figures 26A and 26B. Photomicrographs showing electron microprobe traverses across samples SC13A-A (A) and SC13B (B). These slides were taken in cross-polarized light so garnet appears black. Note the blade-like inclusions of sillimanite and xenoblastic quartz inclusions in each garnet.

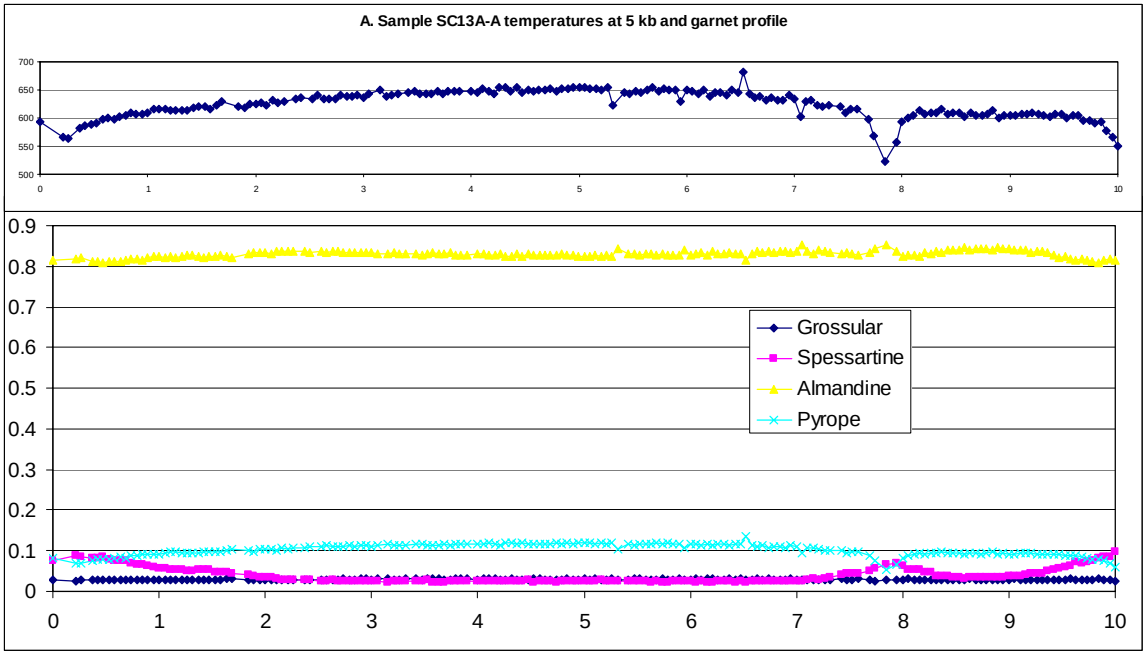

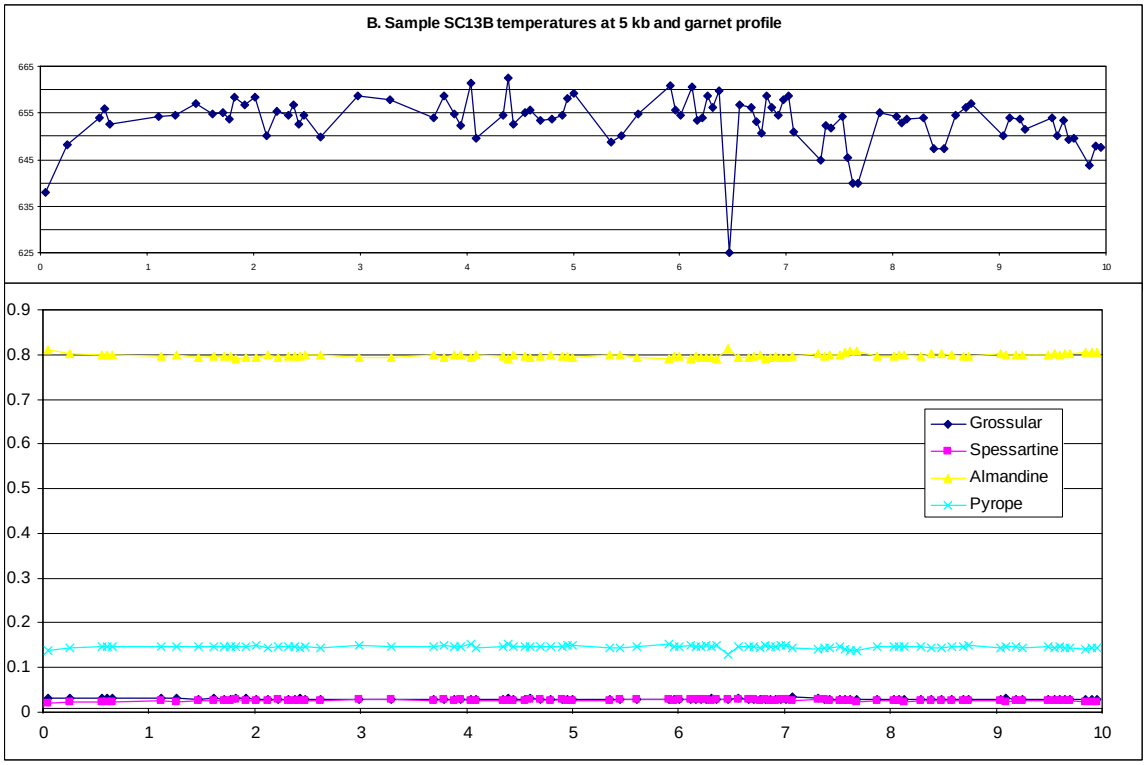

Figures 27A and 27B. Charts showing compositions and calculated temperatures (Holdaway, 2000) across each garnet profile at 5 kb. Markers in profiles correspond with each analyzed point.

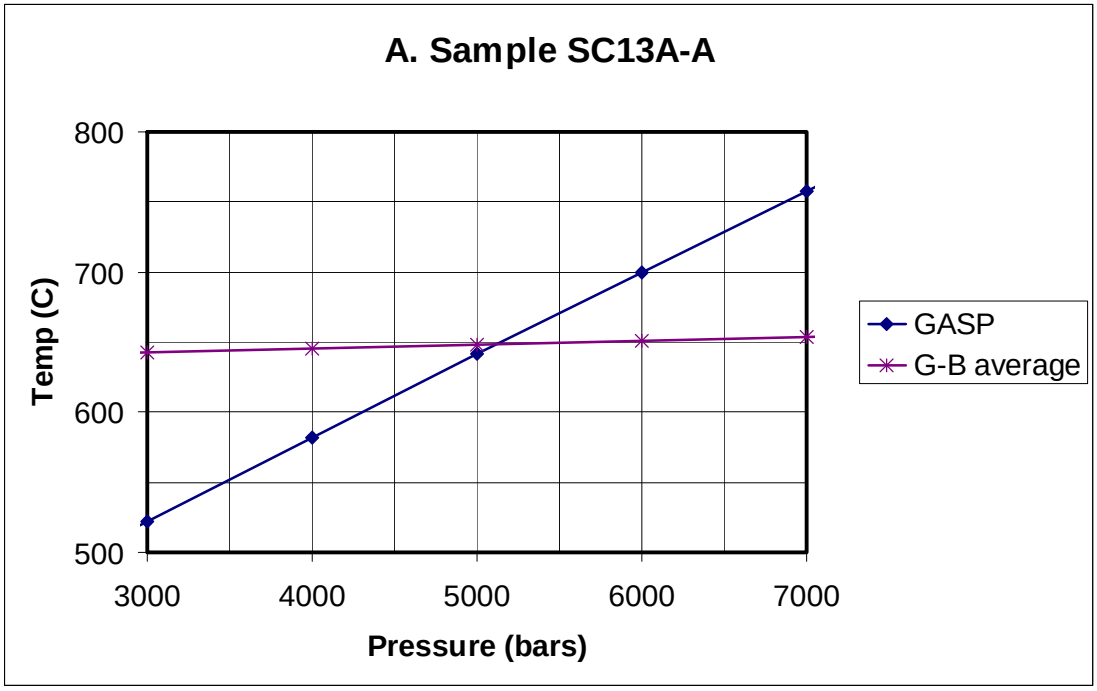

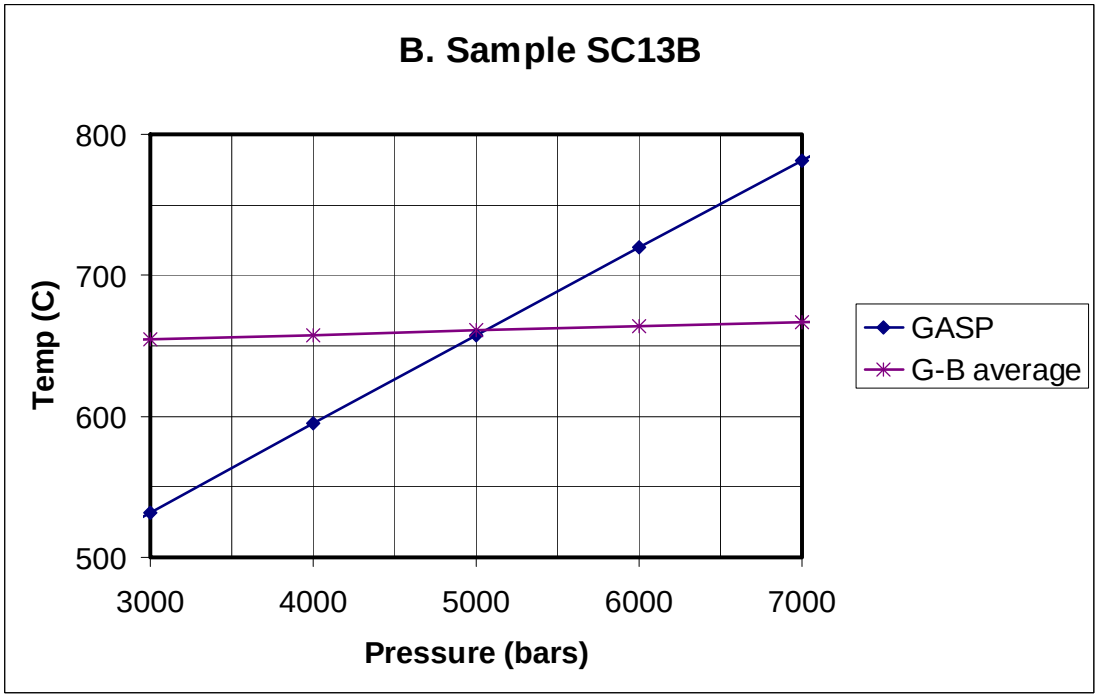

Figures 28A and 28B. Pressure-temperature diagrams showing lines produced by GASP barometry (Holdaway, 2001) and garnet-biotite thermometry (Holdaway, 2000). The intersection of the lines represents the peak metamorphic conditions of the sample in P-T space. Figure 28A represents the approximate P-T conditions of sample SC13A-A, 653^{o} C and 5226 bars. Figure 28B represents the approximate P-T conditions of sample SC13B, 661^{o} C and 5071 bars.

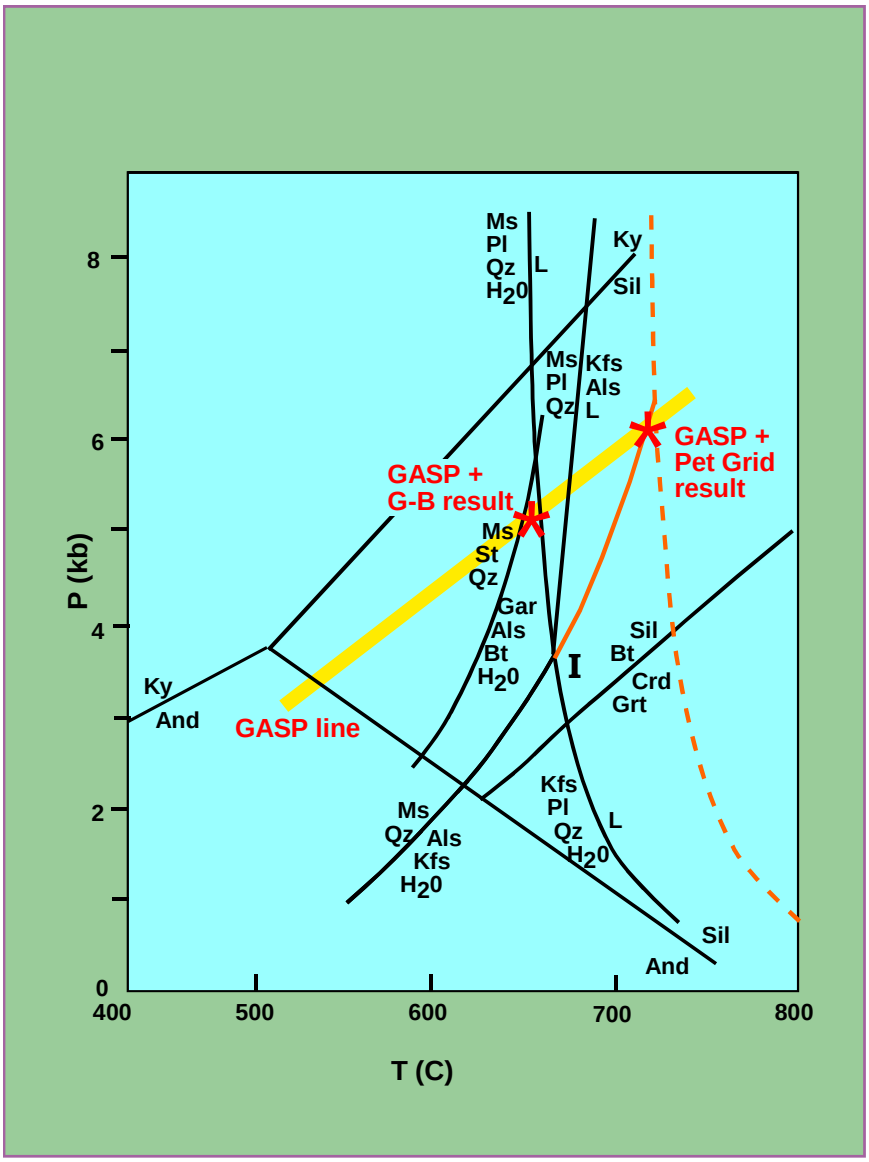

Figure 29. Petrogenetic grid showing simplified KNaFMASH system (Frost and Tracy, 1991). The mineralogy of samples SC13A-A and SC13B from the study area restricts them to the area on the high temperature side of the Ms+Qz→Als+Kfs+H_20 reaction because the rocks contain no prograde muscovite, but do contain sillimanite and K feldspar, and the area on the low temperature side of the Kfs+Pl+Qz+H_20→L reaction because the rocks do not contain definitive evidence of liquid melt. Note the placement of the Kfs+Pl+Qz+H_20→L reaction is appropriate only for end-member albite and as the An percentage increases in plagioclase, the Kfs+Pl+Qz+H_20→L reaction migrates to the right. The approximate position of the reaction using a plagioclase composition of An_{20} is represented by a dashed orange line. The invariant point (I) migrates along the reaction Ms+Qz→Als+Kfs+H_20 (represented by a solid orange line) with increasing Ca in the system. The thick yellow line is the result yielded by GASP barometry. The left star represents the P-T conditions of GASP plus garnet-biotite thermometry. The right star represents the P-T conditions determined by the intersection of the GASP line and the line representing the sillimanite- and K feldspar-producing reaction.

their maximum metamorphic temperatures. Combining the use of quantitative P-T techniques and the use of petrogenetic grids, the peak metamorphic conditions of samples SC13A-A and SC13B appear to be 650°-720° C and 5.1-6.2 kilobars.

Implications

Peak metamorphic pressures and temperatures are moderate- to high-grade throughout the northern Hualapai Mountains and similar to the Cerbat Mountains to the north (this study; Duebendorfer et al., 2001a, b). No unequivocal evidence of melting was found in the northern Hualapai Mountains, but metamorphic rocks in the Cerbat Mountains were locally melted (Duebendorfer et al., 2001a). The lack of melting in the northern Hualapai Mountains indicates that either the metamorphic conditions there were uniformly lower than in the Cerbat Mountains or fluid conditions were different, but the temperatures recorded in the Hualapai Mountains (650°-720° C) are only slightly below the melting temperature for the mineral assemblage found there. Therefore, there is no need for a metamorphic boundary between the Hualapai Mountains and the Cerbat Mountains.

CHAPTER 5: TECTONIC IMPLICATIONS

Deformational events in northwestern Arizona

Several studies in northwestern Arizona have documented evidence for two Paleoproterozoic deformational events (e.g., Karlstrom and Bowring, 1988; Duebendorfer et al., 2001a). The first is referred to as D_1 and is exposed across central and northwestern Arizona as a northwest-striking and moderately to shallowly dipping metamorphic foliation. This event is generally considered to have occurred prior to 1735 Ma, but could be as young as 1720 Ma (e.g., Karlstrom and Bowring, 1988; Albin and Karlstrom, 1991; Ilg et al., 1996; Duebendorfer et al., 2001a). A northeast-southwest shortening direction is required to produce the northwest-striking foliation and this fabric has been interpreted to represent a pre-Yavapai orogeny collision between the Mojave and Yavapai provinces (Duebendorfer et al., 2001a).

The later fabric is referred to in this study as D_3 (it has been previously referred to as D_2) and is a steeply-dipping northeast-striking metamorphic foliation present throughout central and northwestern Arizona. This event is generally considered to have occurred between 1700 and 1680 Ma (e.g., Karlstrom and Bowring, 1988; Albin and Karlstrom, 1991; Ilg et al., 1996; Duebendorfer et al., 2001a). A northwest-southeast shortening direction is required to produce this northeast-striking foliation and this fabric is thought to represent the Yavapai orogeny, a collision between the combined Mojave-Yavapai provinces and the older rocks of North America to the north (e.g., Karlstrom and Bowring, 1988; Duebendorfer et al., 2001a).

This study has identified a foliation associated with a newly-recognized event temporally intermediate between D_1 and D_3. This north- to northwest-striking steeply

dipping foliation can be seen overprinting D_1 and being reoriented by D_3 in the same outcrop (Figure 17). Preliminary dating of the Paleoproterozoic orthogneiss unit constrains the timing of S_2 fabric development to be 1717 Ma or younger (K. Chamberlain, personal communication, 2003). This date places the fabric temporally later than the D_1 deformational period and earlier than the D_3 deformational period. Rocks younger than 1717 Ma have not been found to strike northwest anywhere else in northwestern Arizona.

The only other study in the region that has also identified three Paleoproterozoic fabrics is that of Quigley et al. (2002) in the North Virgin Mountains, southern Nevada. These authors interpret northwest-trending inclusion trails in porphyroblasts as evidence for D_1, a north-northwest striking foliation as evidence for D_2, and a northeast-striking foliation as evidence for D_3. The orientations of these three fabrics are geometrically equivalent to fabric orientations in the northern Hualapai Mountains, however, Quigley et al. (2002) did not report any radiometric dates to constrain timing of any of the fabrics exposed in the North Virgin Mountains.

The presence of two areas with geometrically similar fabrics within ~200 km, one of which has not been previously recognized, suggests that this study and that of Quigley et al. (2002) may have documented a fabric that could have been overlooked in other studies. However, it must be considered that other studies in the region may not have overlooked any Paleoproterozoic fabrics and the geometric similarities between the fabrics of Quigley et al. (2002) and this study are coincidental. It is important to note that in the study of Quigley et al. (2002) D_1 is represented only by inclusion trails within porphyroblasts, a fabric that is arguably less significant than the strong foliation present

in the Hualapai and Cerbat ranges. It is also important to note that in the northern Hualapai Mountains D_2 is represented by two areas of overprinting fabric relations. The north-striking fabric orientations at these two areas could possibly be explained by partial rotation of D_1 into D_3 and that fabrics related to those two deformations are more heterogeneous in orientation that previously thought. The north-trending D_2 fold axes in the southern part of the study area might represent an early phase of the D_3 deformational event.

Most northwest-striking fabrics in the study area are interpreted to be related to D_1 because of their similarities in orientation to fabrics that have been dated as D_1 in the Cerbat Mountains. The age of the northwest-striking foliation in the northern Hualapai Mountains is not known, however, so it is possible that the northwest-striking foliation in the northern Hualapai Mountains is related to the newly recognized D_2 episode, which has been constrained to post-1717 Ma. The presence of three separate foliations in a small area in the southern part of the study area (near station 56, see Plate 3) suggests that some D_1 fabric exists in the study area, but without more geochronological data it is not possible to know how much.

The Gneiss Canyon shear zone and the Mojave-Yavapai boundary

The Gneiss Canyon shear zone, a proposed structural, metamorphic, and isotopic boundary, has been projected southwest from its exposure in the Lower Granite Gorge of the Grand Canyon into the northern Hualapai Mountains within the present study area (Albin and Karlstrom, 1991; K. Karlstrom, personal communication, 2003) (Figure 2). However, the structural and metamorphic data collected in this study, discussed in the

Chapters 3 and 4, and reviewed briefly below, do not support the presence of the Gneiss Canyon shear zone in the study area.

A strong, steeply-dipping, northeast-striking metamorphic foliation associated with the Gneiss Canyon shear zone has been recognized in the Lower Granite Gorge. Rocks containing this foliation are dominantly LS tectonites with uniform shear sense indicating northwest-side-up, reverse-sense movement across the shear zone (Albin and Karlstrom, 1991; K. Karlstrom, personal communication, 2003). A metamorphic gradient has been recognized across the shear zone as well, with amphibolite facies rocks to the southeast and granulite facies rocks to the northwest of the shear zone (Robinson, 1994). Robinson (1994) found low-Ca amphibolites east of the Gneiss Canyon shear zone containing various combinations of cummingtonite, anthophyllite, gedrite, garnet, and cordierite. Low-K pelitic schists with quantitative temperature and pressure ranges of 550-600^{o} C and 2.5-3.5 kb are also present east of the shear zone. Robinson (1994) used the garnet-biotite thermometer of Williams and Grambling (1990) and the GASP barometer of Koziol and Newton (1988) and Hodges and Crowley (1985) to obtain the quantitative pressure and temperature data. The low-K pelitic schists contain one of two assemblages: quartz, biotite, garnet, staurolite, plagioclase, and sillimanite ± muscovite, or quartz, biotite, andalusite, sillimanite, and muscovite. West of the shear zone, Robinson (1994) reported pelitic rocks that contain the assemblage cordierite, biotite, sillimanite, and garnet. Fine-grained muscovite was interpreted to be retrograde. Quantitative temperature and pressure ranges for that area were calculated to be 650-700^{o} C and 3.5-4.5 kb using the garnet-biotite thermometer of Williams and Grambling (1990)

corrected for Ti and Al in biotite, the GASP barometer of Koziol and Newton (1988), and the garnet-biotite-plagioclase-quartz barometer of Hoisch (1990).

In the northern Hualapai Mountains, most of the deformational fabrics record only flattening strains, as indicated by the predominance of S tectonite fabrics. Only 21 kinematic indicators were found in the present study area and these most commonly indicate northwest-side-up shear. Pelitic rocks within and near the present study area yielded lower granulite-facies pressures and temperatures. Pelitic assemblages within the study area contain sillimanite + K feldspar in the absence of prograde muscovite. Quantitative temperature and pressure ranges for pelites within the study area are 650-720^{o} C and 5.1-6.2 kb. These pressure-temperature conditions are only slightly lower than the conditions of metamorphism in the Cerbat Mountains, to the north, indicating a sharp metamorphic boundary is not present between the Hualapai and Cerbat ranges.

The Gneiss Canyon shear zone has been proposed to be a crustal boundary in northwestern Arizona, but there may be no need for such a boundary in that location. The Crystal shear zone in the Upper Granite Gorge of the Grand Canyon has been recognized as the boundary between Mojave-type and Yavapai-type Pb isotopic signatures (Hawkins et al., 1996) as well as a possible structural boundary (Ilg et al., 1996). The Crystal shear zone is on trend with a Pb isotopic gradient near Bagdad, Arizona, that has also been identified as the easternmost extent of Mojave-type crust (Wooden and DeWitt, 1991). Therefore, all areas west of this boundary should be part of the Mojave province. The complication is that an area of mixed isotopic character, including some pockets of juvenile ("Yavapai-like") crust, has been identified in a 75-km "boundary zone", the eastern margin of which is thought to trend from near Bagdad,

Arizona, to the Crystal shear zone in the Upper Granite Gorge of the Grand Canyon (Wooden and DeWitt, 1991; Hawkins et al., 1996; Figure 3). If the "boundary zone" is a separate tectonic block, it could be bounded by the Gneiss Canyon shear zone on its west margin, as suggested by K. Karlstrom (personal communication, 2003). The western margin of the isotopically mixed boundary zone may not necessarily be marked by a shear zone, however. One alternative possibility is that the isotopically mixed zone may be a narrow part of the Mojave province that was tectonically thinned due to a pre-Yavapai orogeny and pre-Mojave-Yavapai collision failed rifting event. In a rift setting, juvenile material having a Pb isotopic signature similar to the Yavapai province would have been produced in the most highly rifted part of the Mojave province. This model could explain why this zone contains Pb signatures more juvenile than Mojave but more evolved than Yavapai characteristics. In this scenario the western margin of the boundary zone does not need to be marked by a shear zone or other structural boundary. If this model is correct, the western margin could in fact be a cryptic (i.e., overprinted by collisional events) system of normal-sense shear zones, the fabric from which must have been overprinted by D_1, D_2, and D_3.

This study fails to provide supporting evidence for the Gneiss Canyon shear zone as a tectonic boundary trending southwest from the Lower Granite Gorge though the northern Hualapai Mountains. The Gneiss Canyon shear zone in the Lower Granite Gorge may represent the western margin of the isotopically mixed zone, however, the western margin of the zone (as defined by Pb isotopic values) does not appear to strike southwest though the study area. Isotopic studies have shown that both the northern Hualapai and Peacock Mountains possess Mojave-like Pb-isotopic signatures. There is a

sharp gradient in Pb isotopic values between these ranges and the Cottonwood Cliffs (more juvenile Pb isotopic signature), that lie immediately east of the Peacock Mountains (Wooden and DeWitt, 1991; K. Chamberlain, unpublished data**;** Figure 3). Similarly, both the northern Hualapai and Peacock Mountains have experienced granulite-facies metamorphism, whereas the grade of regional metamorphism in the Cottonwood Cliffs is greenschist (Evans, 1999; James et al., 2001; Figure 30). This change in metamorphic grade between the Peacock Mountains and Cottonwood Cliffs occurs over too small of a distance (~8 km) to be explained by a regional increase in metamorphic grade to the west, even if a vertical crustal section were present between the two ranges. This abrupt gradient in metamorphic grade suggests the presence of a structure and possibly represents a new alignment for the Gneiss Canyon shear zone. Together, these observations suggest that the western margin of the "boundary zone" may strike south from the Lower Granite Gorge, rather than southwest (Figure 31).

Another possible tectonic explanation for the orientation of the western margin of the isotopically mixed boundary zone is that it may be related to a transpressional suture. The Shylock shear zone in central Arizona trends north-south and has been interpreted to be the suture between the Big Bug block and the Ash Creek block, both within the Yavapai province (Figure 2; Karlstrom and Bowring, 1993). The Shylock shear zone contains features characteristic of both dip-slip and strike-slip shear zones coeval with plutonism and has been interpreted to represent oblique convergence. The presence of a transpressional setting could explain why the boundary zone margin and possible structure is oriented north-south and obliquely to the major deformational fabrics in the area.

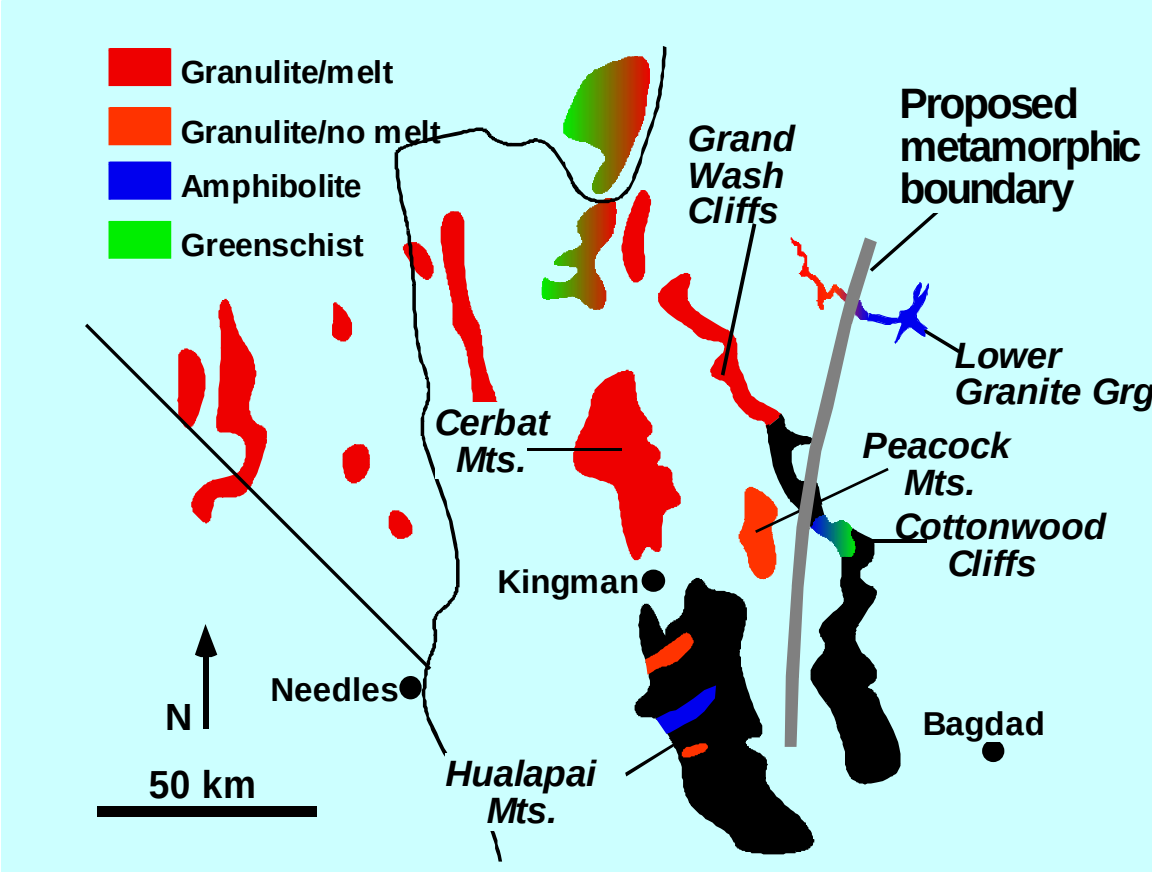

Figure 30. Map showing metamorphic grade in each mountain range in northwestern Arizona. Note that both the northern Hualapai Mountains and the Cerbat Mountains contain granulite facies rocks, whereas the Cottonwood Cliffs contain amphibolite and greenschist facies rocks.

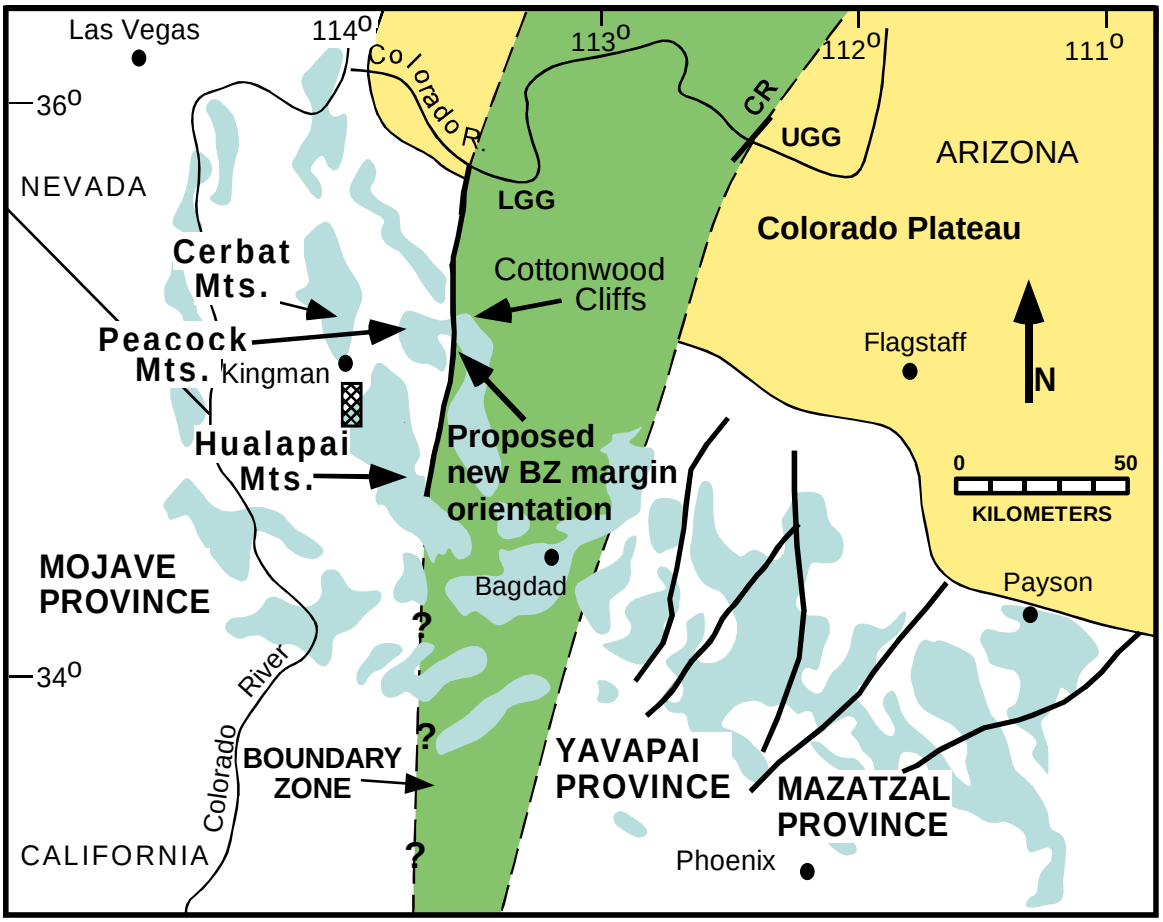

Figure 31. Generalized map of northwestern Arizona showing the proposed new orientation of the boundary zone margin. This new boundary zone margin may also represent the orientation of the Gneiss Canyon shear zone. Question marks represent areas that require further research. For an explanation of abbreviations and other map features please see Figure 2.

Other studies support the hypothesis that the western margin of the isotopically mixed zone may strike north-south. Tertiary and Quaternary basalts in southern Utah have different Nd and Pb isotopic characteristics on either side of a north-south line near the current location of the Hurricane fault (Smith et al., 1999). Smith et al. (1999) proposed that this could represent an older lithospheric boundary. The proposed isotopic boundary of Smith et al. (1999) nearly corresponds with the Nd and Pb isotopic boundaries set forth in two earlier studies (Figure 32). Wooden and DeWitt (1991) identified a boundary separating two Pb isotopic provinces that passes just to the east the study area of Smith et al. (1999), and Bennett and DePaolo (1987) identified a boundary separating two Nd isotopic provinces just to the west of the boundary of Smith et al. (1999).

The Pb isotopic boundary of Wooden and DeWitt (1991) and the Hurricane fault both trend southward toward Gneiss Canyon in the Lower Granite Gorge (whereas the proposed Gneiss Canyon shear zone trends southwest from the Lower Granite Gorge) and the Nd isotopic boundary of Bennett and DePaolo (1987) trends southward toward the present study area. Although the boundaries of Bennett and DePaolo (1987) and Wooden and DeWitt (1991) were based on a limited number of data points, the proximity of the study area of Smith et al. (1999) to these two isotopic boundaries indicates that Smith et al. (1999) may have recognized the northern extension of the western margin of the isotopically mixed zone.

Another study, in the northern Dome Rock Mountains and southern Plomosa Mountains in southwestern Arizona, established that rocks in that area have Mojave province isotopic character and that the Mojave-Yavapai boundary must lie east of these

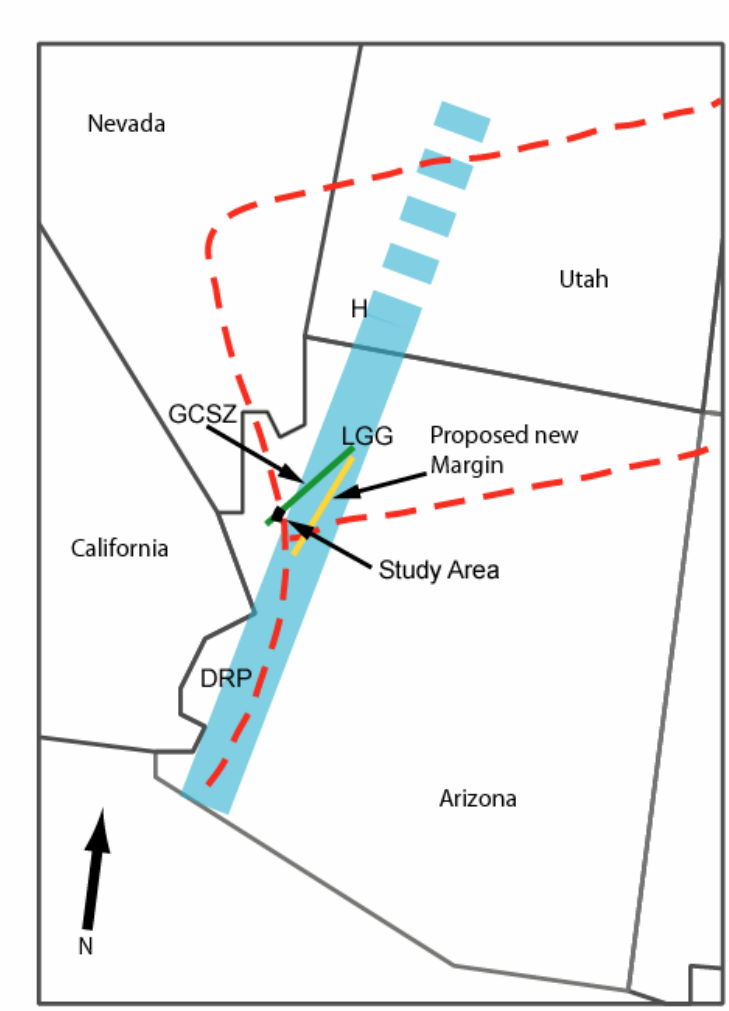

Figure 32. Map showing Arizona and surrounding states. Red dotted lines represent the Nd isotopic province boundaries of Bennett and DePaolo (1987). The thick blue line represents the Pb isotopic boundary of Wooden and DeWitt (1991). The thin green line represents the projected trace of the Gneiss Canyon shear zone ("GCSZ") of Albin and Karlstrom (1991). The thin yellow line represents the proposed new western margin of the boundary zone. The Dome Rock and Plomosa Mountains of Lerch et al. (1991) are represented by "DRP". The town of Hurricane, Utah and the study area of Smith et al. (1999) is represented by "H". The Lower Granite Gorge of the Grand Canyon is represented by "LGG".

ranges (Figure 32; Lerch et al., 1991). Lerch et al. (1991) further supported the hypothesis that the western boundary of the isotopically mixed zone may trend north-south, because a structure (e.g., the Gneiss Canyon shear zone) trending southwest from the Lower Granite Gorge would lie considerably west of the Dome Rock and Plomosa Mountains (Figure 32).

CHAPTER 6: CONCLUSIONS

Summary

The northern Hualapai Mountains are located in an area of northwestern Arizona proposed to be part of the boundary zone between the Mojave and Yavapai Proterozoic crustal provinces. The goal of this study was to perform detailed reconnaissance mapping in an area that had never been mapped geologically and to gather structural and metamorphic data to assess models for Paleoproterozoic tectonics in the area. The following are the conclusions of this study:

- I have identified a Paleoproterozoic fabric temporally intermediate between the northwest-striking S_1 and the northeast-striking S_3. This fabric is present in at least two places in the study area and its age is constrained to post-1717 Ma and pre-D_3. This fabric, S_2, consists of a north- to northwest-striking metamorphic foliation and similarly oriented mesoscopic cylindrical fold axes. The S_2 fabric clearly overprints the S_1 fabric and is reoriented by the S_3 fabric.
- Paleoproterozoic structures in the study area are similar in orientation to those present in the Gneiss Canyon shear zone in the Lower Granite Gorge, but lack the strong kinematic indicators and widespread migmatitic textures common in the Lower Granite Gorge. Rocks in the northern Hualapai Mountains are primarily S tectonites, an observation that is not consistent with the presence of a major crustal shear zone in the vicinity.
- I obtained quantitative pressure and temperature values for two samples in the study area using garnet-biotite geothermometry and GASP geobarometry. Based on combined thermobarometric data and petrogenetic grids, peak metamorphic

temperatures ranged from approximately 650°-720° C and peak metamorphic pressures ranged from 5.1-6.2 kb. These P-T conditions are similar to both the Cerbat Mountains to the north and the Hualapai Mountains south of the study area. These data illustrate that there is no need for a metamorphic boundary near the study area, but a metamorphic gradient is present farther east.

- The Pb isotopic signature near the study area is Mojave-like, as is the Pb isotopic signature in the Cerbat Mountains to the north and the Hualapai Mountains to the south. These data illustrate that there is no Pb isotopic boundary near the study area, but a gradient is present farther east.
- Based on the above conclusions, I propose that the western margin of the Mojave/Yavapai boundary zone (and possibly the Gneiss Canyon shear zone) is east of study area and trends south rather than southwest from the Lower Granite Gorge (Figure 31).

REFERENCES CITED

Albin, A.L., 1991, Structural geology of the Gneiss Canyon shear zone in the Peacock Mountains and southern Grand Wash Cliffs, northwestern Arizona [M.S. thesis]: Flagstaff, Northern Arizona University, 68 p.

Albin, A.L., and Karlstrom, K.E., 1991, Orthogonal Proterozoic fabrics in northwestern Arizona: Multiple orogenic events or progressive deformation during continental assembly, *in* Karlstrom, K.E., ed., Proterozoic geology and ore deposits of Arizona: Arizona Geological Society Digest, v. 19, p. 67-84.

Anderson, J.L., 1983, Proterozoic anorogenic granite plutonism of North America, *in* Medaris, L.G., Jr., Byers, C.W., Mickelson, D.M., and Shanks, W.C., ed., Proterozoic geology: selected papers from an international Proterozoic symposium: Geological Society of America Memoir 161, p. 133-154.

Anderson, J.L., and Bender, E.E., 1989, Nature and origin of Proterozoic A-type granitic magmatism in the southwestern United States of America: Lithos, v. 23, p. 19-52.

Anderson, J.L., Wooden, J.L. and Bender, E.E., 1993, Mojave province of southern California and vicinity, *in* Van Schmus, W.R., et al., 1993, Transcontinental Proterozoic provinces, *in* Reed, J.C., Jr., et al., eds., Precambrian: Conterminous U.S.: Boulder Colorado, Geological Society of America, The Geology of North America, v. C-2, p. 176-188.

Barth, A.P., Wooden, J.L., Coleman, D.S., and Fanning, C.M., 2000, Geochronology of the Proterozoic basement of southwesternmost North America, and the origin and evolution of the Mojave crustal province: Tectonics, v. 19, p. 616-629.

Beard, L.S., 1996, Paleogeography of the Horse Spring Formation in relation to the Lake Mead fault system, Virgin Mountains, Nevada and Arizona: Geological Society of America Special Paper, v. 303, p. 27-60.

Bennett, V., and DePeolo, D.J., 1987, Proterozoic crustal history of the western United States as determined by neodymium isotopic mapping: Geological Society of America Bulletin, v. 99, p. 674-685.

Bickford, M.E., and Anderson, J.L., 1993, Middle Proterozoic Magmatism, *in* Van Schmus, W.R., et al., 1993, Transcontinental Proterozoic provinces, *in* Reed, J.C., Jr., et al., eds., Precambrian: Conterminous U.S.: Boulder Colorado, Geological Society of America, The Geology of North America, v. C-2, p. 281-292.

Bohannon, R.G., 1984, Nonmarine sedimentary rock of Tertiary age in the Lake Mead region, southeastern Nevada and northwestern Arizona: U.S. Geological Survey Professional Paper 1259.

Chamberlain, K.R., 1998, Medicine Bow orogeny: Timing of deformation and model of crustal structure produced during continent-arc collision, ca. 1.78 Ga, southeastern Wyoming: Rocky Mountian Geology, v. 33, p. 259-277.

Dann, J.C., 1997, Pseudostratigraphy and origin of the Early Proterozoic Payson ophiolite, central Arizona: Geological Society of America Bulletin, v. 109, p. 347-365.

Duebendorfer, E.M. and Houston, R.S., 1987, Proterozoic accretionary tectonics at the southern margin of the Archean Wyoming craton: Geological Society of America Bulletin, v. 98, p. 554-568.

Duebendorfer, E.M., Chamberlain, K.R., and Jones, C.S., 2001a, Paleoproterozoic tectonic history of the Cerbat Mountains, northwestern Arizona: Implications for crustal assembly in the southwestern United States: Geological Society of America Bulletin, v. 113, p. 575-590.

Duebendorfer, E.M., Hoisch, T.D., and Chamberlain, K.R., 2001b, Structural and metamorphic similarities between Proterozoic rocks in the Cerbat and Hualapai Mountains, northwestern Arizona: Geological Society of America Abstracts with Programs, v. 33, no. 5, p. 33.

Duebendorfer, E.M., 2003, The interpretation of stretching lineations in multiply deformed terranes: an example from the Hualapai Mountains, Arizona, USA: Journal of Structural Geology, v. 25, p. 1393-1400.

Emslie, R.F., 1978, Anorthosite massifs, rapakivi granites, and Late Proterozoic rifting of North America: Precambrian Research, v. 7, p. 647-650.

Evans, P.J.F.E., 1999, Proterozoic structure and geology of the Cottonwood Cliffs, Mohave County, Arizona [M.S. thesis]: Flagstaff, Northern Arizona University, 176 p.

Ferguson, C.B., 2002, Deformation associated with the 1.4 Ga Boriana Canyon pluton, northwestern Arizona: Regional strain or magma emplacement? [M.S. thesis]: Flagstaff, Northern Arizona University, 113 p.

Frost, R., and Tracy, R.J., 1991, Phase equilibria and thermobarometry of metapelites, *in* Kerrick, D.M., ed., Contact Metamorphism: Mineralogical Society of America, Reviews in Mineralogy, v. 26, p. 105.

Hawkins, D.P., Bowring, S.A., Ilg, B.R., Karlstrom, K.E., and Williams, M.L., 1996, U-Pb geochronologic constraints on the Paleoproterozoic crustal evolution of the Upper Granite Gorge, Grand Canyon, Arizona: Geological Society of America Bulletin, v. 108, p. 1167-1181.

Hodges, K.V., and Crowley, P.D., 1985, Error estimation and empirical geothermometry for pelitic systems: American Mineralogist, v. 70, p. 702-709.

Hoisch, T.D., 1990, Empirical calibration of six geobarometers for the mineral assemblage quartz+muscovite+biotite+plagioclase+garnet: Contributions to Mineralogy and Petrology, v. 104, p. 225-234.

Holdaway, M.J., 2000, Application of new experimental and garnet Margules data to the garnet-biotite geothermometer: American Mineralogist, vol. 85, p. 881-892.

Holdaway, M.J., 2001, Recalibration of the GASP geobarometer in light of recent garnet and plagioclase activity models and versions of the garnet-biotite geothermometer: American Mineralogist, vol. 86, p. 1117-1129.

Ilg, B.R., Karlstrom, K.E., Hawkins, D.P., and Williams, M.L., 1996, Tectonic evolution of Paleoproterozoic rocks in the Grand Canyon: Insights into middle-crustal processes: Geological Society of America Bulletin, v. 108, p. 1149-1166.

James, S.C., Duebendorfer, E.M., and Hoisch, T.D., 2001, Location of the granulite-amphibolite facies transition in northwestern Arizona: Geological Society of America Abstracts with Programs, v. 33, no. 5, p. 24.

Jones, C.S., 1998, Proterozoic geologic history of the Vock Canyon area, Cerbat Mountains, northwestern Arizona [M.S. thesis]: Flagstaff, Northern Arizona University, 125 p.

Karlstrom, K.E., and Houston, R.S., 1984, The Cheyenne belt: Analysis of a Proterozoic suture in southern Wyoming: Precambrian Research, v. 25, p. 415-446.
Karlstrom, K.E., and Bowring, S.A., 1988, Early Proterozoic assembly of tectonostratigraphic terranes in southwestern North America: Journal of Geology, v. 96, p. 561-576.
Karlstrom, K.E., and Bowring, S.A., 1991, Styles and timing of Early Proterozoic deformation in Arizona: Constraints on tectonic models, *in* Karlstrom, K.E., ed., Proterozoic geology and ore deposits of Arizona: Arizona Geological Society Digest, v. 19, p. 1-10.
Karlstrom, K.E., and Bowring, S.A., 1993, Proterozoic orogenic history of Arizona, *in* Van Schmus, W.R., et al., 1993, Transcontinental Proterozoic provinces, *in* Reed, J.C., Jr., et al., eds., Precambrian: Conterminous U.S.: Boulder Colorado, Geological Society of America, The Geology of North America, v. C-2, p. 188-211.
Karlstrom, K.E., and the CD-ROM Working Group, 2002, Structure and evolution of the lithosphere beneath the Rocky Mountains: Initial results from the CD-ROM experiment: GSA Today, v. 12, no. 3, p. 4-10.
Karlstrom, K.E., and Morgan, P., 1988, Undergraduates take to the field: Geotimes, Dec. 1988, p. 8-10.
Kessler, E.J., 1976, Rb-Sr geochronology and geochemistry of Precambrian rocks of the northern Hualapai Mountains, Mojave County, Arizona [M.S. thesis]: Tucson, University of Arizona, 73 p.
Koziol, A.M., and Newton, R.C., 1988, Redetermination of the anorthite breakdown reaction and improvement of the plagioclase-garnet-Al_2SiO_5-quartz geobarometer: American Mineralogist, v. 73, p. 216-223.
Lerch, M.F., Patchett, P.J., and Reynolds, S.J., 1991, Sr and Nd isotopic studies of Proterozoic rocks in west-central Arizona: Implications for Proterozoic tectonics, *in* Karlstrom, K.E., ed., Proterozoic geology and ore deposits of Arizona: Arizona Geological Society Digest, v. 19, p. 51-56.
Nielson, J.E., Lux, D.R., Dalrymple, G.B., and Glazner, A.F., 1990, Age of the Peach Springs Tuff, southeastern California and western Arizona: Journal of Geophysical Research, v. 95, p. 571-580.
Nyman, M.W., Karlstrom, K.E., Kirby, E., and Graubard, C.M., 1994, Mesoproterozoic contractional orogeny in western North America; evidence from ca. 1.4 Ga plutons: Geology, v. 22, p. 901-904.
Orr, T.R., 1997, Proterozoic structure and geology of the northern Cerbat Mountains, Mojave County, Arizona [M.S. Thesis]: Flagstaff, Northern Arizona University, 90 p.
Passchier, C.W., and Trouw, R.A.J., 1996, Microtectonics: Berlin, Springer-Verlag, 289 p.
Quigley, M.C., Karlstrom, K.E., Beard, S., and Bohannon, B., 2002, Influence of Proterozoic and Laramide structures on the Miocene extensional strain field, North Virgin Mountains, Nevada/Arizona: U.S. Geological Survey Open-File Report 02–172, p. 85-104.

Rhys-Evans, G., 2003, A structural analysis of Walnut Canyon, Hualapai Mountains, northwestern Arizona with reference to Proterozoic tectonics [B.S. thesis]: Flagstaff, Northern Arizona University, 41 p.

Robinson, K., 1994, Metamorphic petrology of the Lower Granite Gorge and the significance of the Gneiss Canyon shear zone, Grand Canyon, Arizona [M.S. thesis]: Amherst, University of Massachusetts, 187 p.

Smith, E.I., Sanchez, A., Walker, J.D., and Wang, K., 1999, Geochemistry of mafic magmas in the Hurricane volcanic field, Utah: Implications for small- and large-scale chemical variability of the lithospheric mantle: Journal of Geology, v. 107, p. 433-448.

Williams, M.L., and Grambling, J.A., 1990, Manganese, ferric iron, and the equilibrium between garnet and biotite: American Mineralogist, v. 75, p. 886-908.

Windley, B.F., 1993, Proterozoic anorogenic magmatism and its orogenic connections: Journal of the Geological Society of London, v. 150, p. 39-50.

Wooden, J.L., and Miller, D.M., 1990, Chronologic and isotopic framework for Early Proterozoic crustal evolution in the eastern Mojave desert region, California: Journal of Geophysical Research, v. 95, p. 20133-20146.

Wooden, J.L., and DeWitt, E., 1991, Pb isotopic evidence for a major Early crustal boundary in western Arizona, *in* Karlstrom, K.E., ed., Proterozoic geology and ore deposits of Arizona: Arizona Geological Society Digest , v. 19, p. 27-50.

Wooden, J.L., Nutman, A.P., Miller D.M., Howard, K.A., Bryant, B., DeWitt, E., and Mueller, P.A., 1994, SHRIMP U-Pb zircon evidence for late Archean and Early Proterozoic crustal evolution in the Mojave and Arizona crustal provinces: Geological Society of America Abstacts with Programs, v. 26, no. 6, p. 69.

Young, R.A., and Brennan, W.J., 1974, Peach Springs tuff: Its bearing on structural evolution of the Colorado Plateau and development of Cenozoic drainages in Mohave County, Arizona: Geological Society of America Bulletin, v. 85, p. 83-90.

Young, R.A., 1979, Laramide deformation, erosion and plutonism along the southwestern margin of the Colorado Plateau: Tectonophysics, v. 61, p. 25-47.

APPENDIX

Table A-1. Table showing information about each kinematic indicator recorded.

Location	Local Foliation	Local Lineation	Directional sense of movement	Relative sense of movement	From field measurement or thin section
Station 4 (WC3)	200, 90	82, 020	NW side up	Vertical	Field
Station 7	243, 85 NW	?*	NW side up	Reverse	Field
Attitude 58	225, 65 NW	65, 310	NW side up	Reverse	Field
Station 12	264, 59 NW	55, 355	NW side up	Reverse	Field
Attitude 67	205, 80 NW	71, 331	NW side up	Reverse	Field
Attitude 76	230, 32 NW	28, 330	NW side up	Reverse	Field
Attitude 84	234, 80 NW	60, 299	SE side up	Normal	Field
Attitude 238	053, 80 SE	?	NW side up + Dextral	Normal	Field
Attitude 329	224, 84 NW	?	SE side up	Normal	Field
Attitude 399	210, 60 NW	60, 330	NW side up	Reverse	Field
Attitude 418	104, 87 SW	?	NE side up	Normal	Field
Attitude 450	245, 65 NW	?	NW side up	Reverse	Field
Attitude 226	244, 90	?	SE side up + Dextral	Vertical	Field
Station 31	228, 83 NW	?	SE side up + Sinistral	Normal	Field
Attitude 519	232, 55 NW	? Down dip	NW side up	Reverse	Field
Attitude 557	204, 70 NW	50, 237	SE side up	Normal	Field
SC1	013, 90	55, 013	SE side up	Vertical	Thin section
SC6	240, 84 NW	70, 036	NW side up	Reverse	Thin section
WC4	293, 45 NE	36, 070	NE side up	Reverse	Thin section
WC8	260, 82 NW	?	NW side up	Reverse	Thin section
WC15A	253, 60 NW	~45^{o}, SW	NW side up	Reverse	Thin section

*A question mark in the lineation column indicates that an exact value is not known. In some cases, a lineation was seen but could not be measured in the field, or its general direction was noted but not measured. In other cases, a lineation could not be measured on the outcrop but an approximation was deduced in the laboratory using a sample oriented by foliation.

Table A-2. Table showing information about each fold measured or observed. The "Constructed" designation in the table indicates that the axis of the fold could not be directly measured in the field, but the orientation of the axis was constructed using stereonets based on limb measurements and axial surface measurements taken in the field.

Location	Axis	Axis measured or constructed	Axial Surface	Description
Station 6	60, 321	Constructed	237, 70 NW	Tight, vertical, outcrop-scale
Station 17	36, 031	Constructed	321, 38 NE	Open, hand sample-scale
Attitudes 175, 176	32, 113	Constructed	108, 81 SW	Closed, map-scale, plunging synform
Attitudes 536, 537	60, 327	Constructed	315, 84 NE	Gentle, map scale, plunging antiform
Station 23	29, 060	Measured	050, 77 SE	Chevron-style, cm-scale
Station 40	68, 244	Measured	unknown	Tight to isoclinal, steeply plunging synform
Attitudes 182, 183	24, 237	Measured	unknown	Gentle, meter-scale
Attitude 274	60, 184	Measured	unknown	Isoclinal, outcrop-scale
Station 49	34, 012	Measured	unknown	Very small Z-type, outcrop-scale
Attitude 417	74, 290	Measured	unknown	Open, outcrop-scale
Attitude 426	08, 315	Constructed	unknown	Open, outcrop-scale
Attitude 431	46, 030	Measured	unknown	Very tight, outcrop-scale
Attitude 531	58, 000	Measured	unknown	Crenulation, outcrop-scale
Station 32	30, 072 53, 070	Measured	unknown	Tight, cm-scale folds
Attitude 206	64, 265	Measured	unknown	Isoclinal, outcrop-scale
Attitude 484	60, 012	Measured	unknown	Crenulation cylindrical, outcrop-scale
Attitudes 528, 529	53, 293	Constructed	unknown	